Experimental Studies of Allene, Methylacetylene, and the Propargyl Radical: Bond Dissociation Energies, Gas-Phase Acidities, and Ion−Molecule Chemistry

Marin S. Robinson,[†,‡] Mark L. Polak,[§,⊥] Veronica M. Bierbaum,*[,†] Charles H. DePuy,*[,†] and W. C. Lineberger*[,§]

Contribution from the Department of Chemistry and Biochemistry, University of Colorado, Boulder, Colorado 80309-0215, and the Joint Institute for Laboratory Astrophysics, University of Colorado and National Institute of Standards and Technology, Boulder, Colorado 80309-0440

Received December 23, 1994[⊗]

Abstract: Electron affinities and ΔH_{acid} are combined in a thermochemical cycle to arrive at bond dissociation energies for allene, methylacetylene, and the propargyl radical: $D_0(CH_2{=}C{=}CH{-}H) = 88.7 \pm 3$ kcal mol^{-1}, $D_0(H{-}CH_2C{\equiv}CH) = 90.3 \pm 3$ kcal mol^{-1}, $D_0(CH_3C{\equiv}C{-}H) = 130.2 \pm 3$ kcal mol^{-1}, and $D_0(CH_2{=}C{=}\dot{C}{-}H) = 100 \pm 5$ kcal mol^{-1}. Electron affinity measurements were determined using negative ion photoelectron spectroscopy and yielded the following for the propargyl, 1-propynyl, and propadienylidene radicals: $EA(CH_2{=}C{=}\dot{C}H) = 0.918 \pm 0.008$ eV, $EA(CH_3C{\equiv}\dot{C}) = 2.718 \pm 0.008$ eV, and $EA(CH_2{=}C{=}\ddot{C}) = 1.794 \pm 0.008$ eV. Gas-phase acidity measurements were made using proton transfer kinetics in a flowing afterglow/selected-ion flow tube and yielded the following for allene, methylacetylene, and the propargyl radical: $\Delta G_{acid}(CH_2{=}C{=}CH{-}H) = 372.8 \pm 3$ kcal mol^{-1}, $\Delta G_{acid}(H{-}CH_2C{\equiv}CH) = 374.7 \pm 3$ kcal mol^{-1}, $\Delta G_{acid}(CH_3C{\equiv}C{-}H) = 373.4 \pm 2$ kcal mol^{-1}, and $\Delta G_{acid}(CH_2{=}C{=}\dot{C}H) = 364 \pm 5$ kcal mol^{-1}. ΔG_{acid} was converted to ΔH_{acid} by employing ΔS_{acid}: $\Delta H_{acid}(CH_2{=}C{=}CH{-}H) = 381.1 \pm 3$ kcal mol^{-1}, $\Delta H_{acid}(H{-}CH_2C{\equiv}CH) = 382.7 \pm 3$ kcal mol^{-1}, $\Delta H_{acid}(CH_3C{\equiv}C{-}H) = 381.1 \pm 3$ kcal mol^{-1}, and $\Delta H_{acid}(CH_2{=}C{=}\dot{C}H) = 372 \pm 5$ kcal mol^{-1}. Evidence is provided for the isomerization of the allenyl anion ($CH_2{=}C{=}CH^-$) to the 1-propynyl anion ($CH_3C{\equiv}C^-$) in the proton transfer reactions of $CH_2{=}C{=}CH^-$ with CH_3OH and CH_3CH_2OH. This complexity limits the precision of experimental measurements. This study explores the intricacies of determining gas phase acidity values by proton transfer reactions for systems in which isomerization can occur.

1. Introduction

Perhaps the most fundamental property of any molecule is its energy or heat of formation. However, for unstable species the determination of such energies can be difficult, and seemingly appropriate experimental measurements are often susceptible to misinterpretation.[1] A case in point involves the CH homolytic bond dissociation energy of acetylene from which one can obtain the heat of formation of the ethynyl radical, $HC{\equiv}\dot{C}$. Different experimental techniques including pyrolysis kinetics,[2−4] spectroscopic identification of predissociation,[5−7] ionization potential[8] and appearance potential determinations,[9] threshold photoionization measurements using synchrotron radiation,[10] and kinetic energy release measurements upon photolysis[11,12] report CH bond dissociation energies ranging from 118 to 135 kcal mol^{-1}. More recently, anion thermochemical cycles,[13] kinetic energy release measurements,[14] and ultraviolet photolysis have arrived at a consensus for the CH bond dissociation energy,[15] measured by Ervin et al.[13] to be $D_0(H{-}C{\equiv}CH) = 131.3 \pm 0.7$ kcal mol^{-1}.

These workers determined this value (eq 4) by use of the following thermochemical cycle (eqs 1−4):

R^-	$\longrightarrow R + e^-$	EA(R)	(1)
RH	$\longrightarrow R^- + H^+$	ΔH_{acid}(RH)	(2)
$H^+ + e^-$	$\longrightarrow H$	−IP(H)	(3)
RH	$\longrightarrow R + H$	D(R−H)	(4)

The cycle includes the electron affinity of C_2H (eq 1), the gas-

† Department of Chemistry and Biochemistry.
‡ Current address: Cooperative Institute for Research in Environmental Science, University of Colorado, Boulder, CO 80309-0216.
§ Joint Institute for Laboratory Astrophysics and Department of Chemistry and Biochemistry.
⊥ Current address: Space and Environment Technology Center, The Aerospace Corporation, Mail Station M5/747, P.O. Box 92957, Los Angeles, CA 90009-2957.

⊗ Abstract published in *Advance ACS Abstracts,* May 15, 1995.

(1) Berkowitz, J.; Ellison, G. B.; Gutman, D. *J. Phys. Chem.* **1994**, *98*, 2744−2765.
(2) Yampol'skii, Yu. P.; Zelentsov, V. V. *React. Kinet. Catal. Lett.* **1981**, *17*, 347.
(3) Frank, P.; Just, T. *Combust. Flame* **1980**, *30*, 231.
(4) Wu, C. H.; Singh, H. J.; Kern, R. D. *Int. J. Chem. Kinet.* **1987**, *19*, 975.
(5) Fuji, M.; Haijima, A.; Ito, M. *Chem. Phys. Lett.* **1988**, *150*, 380.
(6) Chen, Y.-Q.; Jonas, D. M.; Hamilton, C. E.; Green, P. G.; Kinsey, J. L.; Field, R. W. *Ber. Bunsenges. Phys. Chem.* **1988**, *92*, 329.
(7) Green, P. G.; Kinsey, J. L.; Field, R. W. *J. Chem. Phys.* **1989**, *91*, 5160. Green, P. G. Ph.D. Thesis, Massachusetts Institute of Technology, Sept 1989.
(8) Ionization potential of C_2H: Okabe, H.; Dibeler, V. H. *J. Chem. Phys.* **1973**, *59*, 2430. Berkowitz, J. *Photodissociation, and Photoelectron Spectroscopy*; Academic: New York, 1979; pp 285−290.
(9) Appearance potential of C_2H^+: Dibeler, V. H.; Walker, J. A.; Rosenstock, H. M. *J. Chem. Phys.* **1973**, *59*, 2264. Norwood, K.; Ng, C. Y. *J. Chem. Phys.* **1989**, *91*, 2898.
(10) Shiromaru, H.; Achiba, Y.; Kimura, K.; Lee, Y. T. *J. Phys. Chem.* **1987**, *91*, 17.
(11) Wodtke, A. M.; Lee, Y. T. *J. Phys. Chem.* **1985**, *89*, 4744.
(12) Segall, J.; Lavi, R.; Wen, Y.; Wittig, C. *J. Phys. Chem.* **1989**, *93*, 7287.
(13) Ervin, K. M.; Gronert, S.; Barlow, S. E.; Gilles, M. K.; Harrison, A. G.; Bierbaum, V. M.; DePuy, C. H.; Lineberger, W. C.; Ellison, G. B. *J. Am. Chem. Soc.* **1990**, *112*, 5750−5759.
(14) Baldwin, D. P.; Buntine, M. A.; Chandler, D. W. *J. Chem. Phys.* **1990**, *93*, 6578.
(15) Mordaunt, D. H.; Ashfold, M. N. R. *J. Chem. Phys.* **1994**, *101*, 2630−2631.

0002-7863/95/1517-6766$09.00/0

phase enthalpy of deprotonation of acetylene (eq 2), and the precisely known ionization potential of the hydrogen atom (eq 3).[16] Electron affinities were measured using negative ion photoelectron spectroscopy and gas-phase acidities were determined using proton transfer kinetics in a flow tube apparatus. In the same study, these techniques were used to determine all possible CH bond dissociation energies resulting from the bond-by-bond dismantling of ethylene.

In the present study we again employ negative ion photoelectron spectroscopy, gas-phase acidity measurements, and the thermochemical cycle shown in eqs 1−4, now to measure the CH bond dissociation energies of selected hydrocarbons containing three carbon atoms. In particular, we determine the CH bond dissociation energies of allene ($D_0(CH_2{=}C{=}CH{-}H)$) and methylacetylene ($D_0(H{-}CH_2C{\equiv}CH)$) to form the propargyl radical ($CH_2{=}C{=}\dot{C}H$), of methylacetylene ($D_0(CH_3C{\equiv}C{-}H)$) to form the 1-propynyl radical ($CH_3C{\equiv}\dot{C}$), and of the propargyl radical ($D_0(CH_2{=}C{=}\dot{C}{-}H)$) to form the propadienylidene diradical ($CH_2{=}C{=}\ddot{C}$). To our knowledge the bond dissociation energies of $CH_3C{\equiv}C{-}H$ and $CH_2{=}C{=}\dot{C}{-}H$ have not been reported previously. The bond dissociation energies for $CH_2{=}C{=}CH{-}H$ and $H{-}CH_2C{\equiv}CH$ have been determined from the combined knowledge of the heats of formation of allene and methylacetylene (Table 1), the hydrogen atom (ΔH_f = 52.103 kcal mol^{-1}),[16] and the propargyl radical ($\Delta H_f = 81.5 \pm 1.0$ kcal mol^{-1} as determined in a shock tube study,[17] by very low pressure pyrolysis (VLPP),[18,19] from electron impact appearance potentials,[20] and as summarized by King[18,19]). These values are $D_0(CH_2{=}C{=}CH{-}H) = 87.7 \pm 1.0$ kcal mol^{-1} and $D_0(H{-}CH_2C{\equiv}CH) = 89.3 \pm 1.0$ kcal mol^{-1}. However, in light of the controversy over the CH bond dissociation energy of acetylene, we believe additional independent measurements of these bond dissociation energies are justified.

This work also includes a detailed investigation of the proton transfer reactions used to determine the gas-phase acidity of allene. Using ion−molecule chemistry, deuterium labeling, and gas-phase kinetics we show that a small percentage of allenyl anions ($CH_2{=}C{=}CH^-$) (**1**) undergo isomerization to 1-propynyl anions ($CH_3C{\equiv}C^-$) (**2**) in the course of proton transfer with methanol and ethanol. Since the possibility of isomerization occurs frequently in proton transfer reactions, we explore this process in depth and evaluate its impact on the gas-phase acidity determination.

We have divided the paper into five major sections. We present electron affinity measurements in section 2 and gas-phase acidity measurements in section 3. The complications introduced by the possibility of isomerization during proton transfer are discussed in the gas-phase acidity section. In the fourth section we combine our experimental results to arrive at radical heats of formation and bond dissociation energies utilizing the thermochemical cycle presented in eqs 1−4. Finally, in section 5 we discuss these values and compare them to previous experimental and theoretical results.

2. Electron Affinity Measurements

The electron affinities of the 1-propynyl ($CH_3C{\equiv}\dot{C}$), propargyl ($CH_2{=}C{=}\dot{C}H$) and propadienylidene ($CH_2{=}C{=}\ddot{C}$) radicals were measured using negative ion photoelectron spectroscopy. The photoelectron spectrometer has been described in detail.[21] Since that description, liquid nitrogen cooling capabilities have been added to the flowing afterglow ion source. Without liquid nitrogen cooling, ions are produced at approximately room temperature. To summarize, a negative ion beam is extracted from the flowing afterglow ion source and the beam is mass selected and crossed with the 351-nm output (3.531 eV) of an argon ion laser. Photoelectrons are emitted according to the equation

$$R^-(v'') + h\nu \rightarrow R(v') + e^-(eKE) \qquad (5)$$

and are energy analyzed with 8-meV (0.18 kcal mol^{-1}) resolution. The adiabatic electron affinity corresponds to the energy required to remove an electron from the ground state (electronic, vibrational, and rotational) of the anion to form the ground state neutral. If an electron energy peak (the origin peak) can be assigned to this process, the adiabatic electron affinity is given by the following: EA = $h\nu$ − eKE. In the figures that follow, we express the photoelectron spectra in units of electron binding energy (eBE = $h\nu$ − eKE), so the electron affinity can be read directly off the spectra. Throughout this work, we will only be concerned with the location of the origin peak for each of the photoelectron spectra; a more detailed analysis and discussion of the spectra will appear in a forthcoming publication.[22]

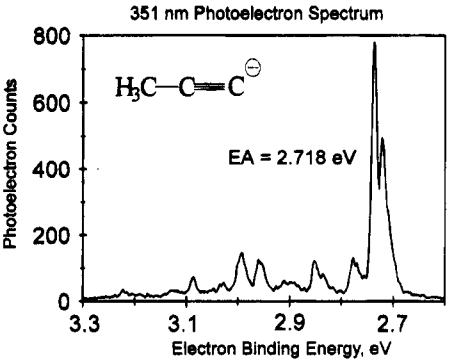

Figure 1. The photoelectron spectrum of the 1-propynyl anion ($CH_3C{\equiv}C^-$) shows transitions to the ^2E ground state of the corresponding radical ($CH_3C{\equiv}\dot{C}$).

Figure 1 shows the photoelectron spectrum of the 1-propynyl anion, $CH_3C{\equiv}C^-$. Previous studies by Oakes and Ellison[23] of the photoelectron spectrum used 488-nm light (2.54 eV) and set a lower bound of 2.60 eV on the electron affinity based on failure to observe a spectrum. We measure an electron affinity of 2.718 ± 0.008 eV from the position of the origin peak, which is the lower electron binding energy peak of the large doublet. The doublet at the origin is due to the split degeneracy of the $^2E(C_{3v})$ ground state of $CH_3C{\equiv}\dot{C}$. This ^2E ground state was predicted in *ab initio* calculations by Bauschlicher and Langhoff[24] using the modified coupled-pair functional method.

The only previous measurement of the propargyl ($CH_2{=}C{=}\dot{C}H$) electron affinity is from photoelectron spectroscopy by Oakes and Ellison,[23] which yielded an electron affinity of 0.893 ± 0.025 eV. However, comparison of their spectra to

(16) Chase, M. W., Jr.; Davies, C. A.; Downey, J. R.; Frurip, D. J.; McDonald, R. A.; Syverud, A. N. *J. Phys. Chem. Ref. Data*, **1985**, *14*, Suppl. No. 1.
(17) Tsang, W. *Int. J. Chem. Kinet.* **1970**, *2*, 23.
(18) King, K. D. *Int. J. Chem. Kinet.* **1978**, *10*, 545.
(19) King, K. D.; Nguyen, T. T. *J. Phys. Chem.* **1979**, *83*, 1940.
(20) Sen Sharma, D. K.; Franklin, J. L. *J. Am. Chem. Soc.* **1973**, *95*, 6562.
(21) Ervin, K. M.; Lineberger, W. C. In *Advances in gas phase ion chemistry*; Adams, N. G., Babcock, L. M., Eds.; JAI: Greenwich, 1992; p 121.
(22) Polak, M. L.; Lineberger, W. C. In preparation, 1994.
(23) (a) Oakes, J. M.; Ellison, G. B. *J. Am. Chem. Soc.* **1983**, *105*, 2969−2975. (b) During the review of this paper we learned of an unpublished value for the gas-phase acidity of allene [$\Delta H_{acid}(CH_2{=}C{=}CH_2)$ = 383.3 kcal mol^{-1}] determined by L. W. Sieck using temperature-dependent equilibrium measurements in an $CH_2{=}C{=}CH_2/C_2H_2$ mixture.
(24) Bauschlicher, C. W.; Langhoff, S. R. *Chem. Phys. Lett.* **1992**, *193*, 380.

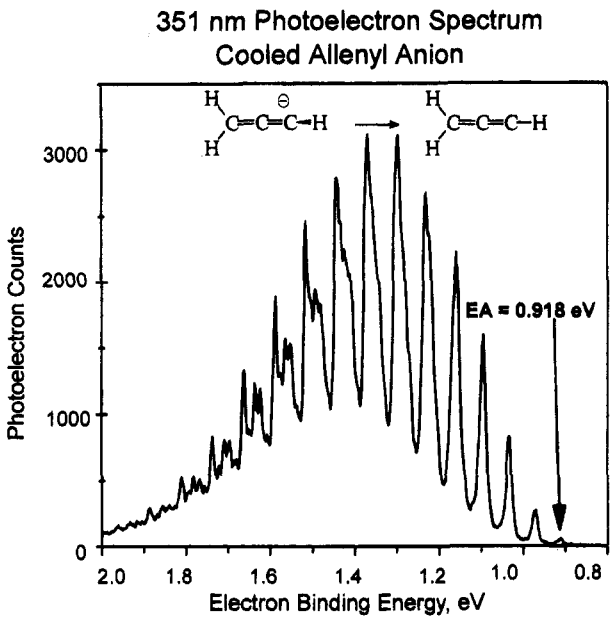

Figure 2. The photoelectron spectrum of the liquid nitrogen cooled allenyl anion (CH_2=C=CH^-) exhibits transitions to the propargyl radical (CH_2=C=$\dot{C}$H). An extended 470-cm^{-1} vibrational progression is observed. The first visible member of the progression is at eBE = 0.918 eV which can be used to determine the electron affinity of CH_2=C=$\dot{C}$H.

those in Figure 2 shows that relatively low resolution and contamination by vibrational hotbands made firm assignment of an origin difficult in the previous effort. Even at higher resolution and cooler vibrational temperatures, the electron affinity of propargyl (CH_2=C=$\dot{C}$H) is difficult to obtain by negative ion photoelectron spectroscopy, because of the large geometry change between the allenyl negative ion (CH_2=C=CH^-) and the propargyl radical photodetachment product. Large geometry changes give rise to low Franck–Condon intensities for the origin transition, making the origin potentially unobservable. Figure 2 displays spectra of the allenyl anion (the anionic form of propargyl) taken with the ion source flow tube cooled with liquid nitrogen. The peak at 0.918 eV electron binding energy is the lowest energy peak that can be firmly assigned as part of the principal vibrational progression (490 cm^{-1}). On this basis, an upper bound can be set to the propargyl electron affinity at 0.918 ± 0.008 eV. The tests described in the next paragraph establish that the electron affinity is in fact 0.918 ± 0.008 eV.

The propargyl (CH_2=C=$\dot{C}$H) electron affinity can be firmly assigned with the use of deuterium substitution and liquid nitrogen cooling. Deuterium substitution is particularly useful because it adds an important constraint to the vibrational origin assignment: the origin peaks for the two spectra should match, except for a small (<0.01 eV) zero-point energy difference. Liquid nitrogen cooling quenches the vibrational energy of the anions, weakening the vibrational hot bands which can obscure transitions from the anion ground state. Consequently, sensitivity to weak transitions from the vibrational ground state is increased. Figure 3 illustrates the liquid nitrogen cooled spectra of allenyl and fully deuterated allenyl. The spectrum of deuterated allenyl displays a vibrational progression at approximately 350 cm^{-1}, and very few peak positions have a corresponding match in the non-deuterated spectrum. The peak at 0.915 eV, however, is a near-perfect match to the 0.918 eV peak already assigned as an upper bound to the electron affinity. In addition, the liquid nitrogen cooling enables us to see that both vibrational progressions come to an abrupt halt at these

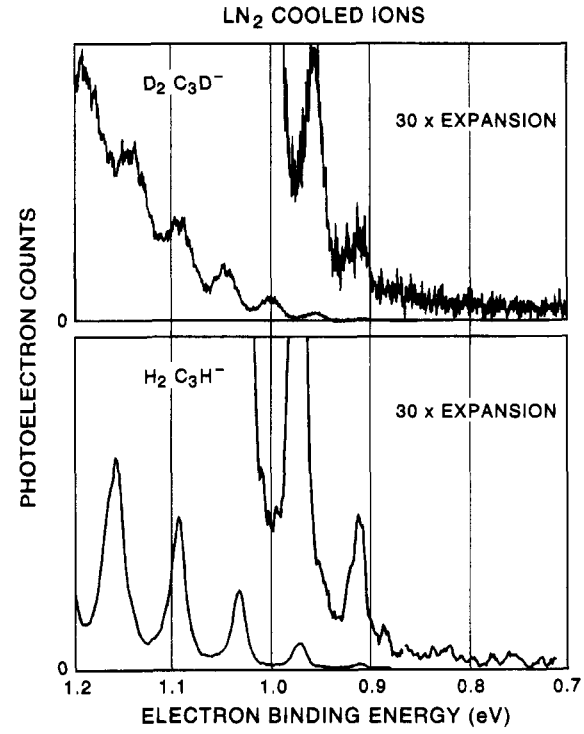

Figure 3. The photoelectron spectra of the liquid nitrogen cooled allenyl (CH_2=C=CH^-) and allenyl-d_3 anions. There is an abrupt end to each vibrational progression at 0.918 eV, and the locations of these peaks in the two spectra are nearly perfectly matched. This match enables assignment of the vibrational origin to this peak.

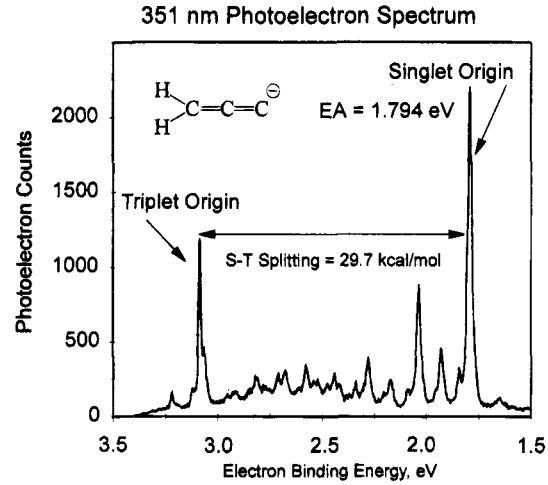

Figure 4. The photoelectron spectrum of the propadienylidene anion (CH_2=C=$\dot{C}^-$) exhibits transitions to both the singlet ground state and triplet excited state of the propadienylidene diradical (CH_2=C=$\ddot{C}$).

peaks. On this basis, the two peaks are assigned as origins, and we obtain EA(CH_2=C=$\dot{C}$H) = 0.918 ± 0.008 eV.

The propadienylidene (CH_2=C=$\ddot{C}$) spectrum (Figure 4) can be interpreted in a straightforward manner. Transitions to both the $^1A_1$ ground state and $^3B_1$ excited state of the propadienylidene diradical are observed. The electron affinity is obtained from the ground state origin peak and is 1.794 ± 0.008 eV, in good agreement with Oakes and Ellison's lower resolution 488-nm spectrum.[25] The 351-nm photon energy in this study permits us to evaluate the propadienylidene singlet–triplet splitting (29.7 ± 0.2 kcal mol^{-1}). This singlet–triplet splitting will prove useful in interpreting our bond dissociation energy results.

(25) Oakes, J. M.; Ellison, G. B. *Tetrahedron* **1986**, *22*, 6263–6267.

3. Gas-Phase Acidity Measurements

A. Introduction. The gas-phase determination of an equilibrium constant (K_{eq}) for a proton transfer reaction of the type

$$R_1^- + R_2H \underset{k_{-6}}{\overset{k_6}{\rightleftharpoons}} R_2^- + R_1H \qquad (6)$$

constitutes an important method for determining the gas-phase acidity of a selected organic reagent, R_2H, relative to an acid of known acidity, R_1H.[26-32] Provided that the forward and reverse processes in eq 6 do not include rearrangements to different ionic or neutral structures during reaction, K_{eq} can be determined by measuring the ratio of the forward and reverse proton transfer rate coefficients or the ratio of the equilibrium product and reactant concentrations:

$$K_{eq} = \frac{k_6}{k_{-6}} = \frac{[R_2^-][R_1H]}{[R_1^-][R_2H]} \qquad (7)$$

The relation $\delta\Delta G_{acid} = \Delta G_{rxn} = -RT \ln K_{eq}$ then yields the gas-phase acidity of R_2H relative to R_1H. Absolute gas-phase acidities (ΔG_{acid}) for R_2H can be obtained from independently known gas-phase acidities for R_1H according to $\Delta G_{acid}(R_2H) = \Delta G_{acid}(R_1H) + \delta\Delta G_{acid}$. ΔG_{acid} can be converted to ΔH_{acid} using the thermodynamic relationship $\Delta H_{acid} = \Delta G_{acid} + T\Delta S_{acid}$.

In this work we describe our efforts to use proton transfer kinetics (k_6/k_{-6}) to determine the gas-phase acidity of allene. However, two factors complicate this determination: the existence of two protonation sites in the allenyl anion ($CH_2{=}C{=}CH^-$) and the possibility of isomerization in the course of the proton transfer reaction. Since proton transfer kinetics are at times used to measure gas-phase acidities in situations where the possibility of isomerization exists, we believed it would be beneficial to examine this complication systematically and to evaluate its impact in light of existing literature and theoretical values. We also employed bracketing techniques to study the reactions of $CH_3C{\equiv}C^-$ and $CH_2{=}C{=}\dot{C}^-$ with selected reference acids and used these results to determine the gas-phase acidities of methylacetylene ($CH_3C{\equiv}C{-}H$) and the propargyl radical ($CH_2{=}C{=}\dot{C}{-}H$), respectively.

B. Experimental. All experiments were performed in the flowing afterglow/selected-ion flow tube (FA-SIFT), described in detail elsewhere.[33] The allenyl ($CH_2{=}C{=}CH^-$), methoxide (MeO^-), and ethoxide (EtO^-) anions were prepared in the first flow tube by allowing their respective parent neutrals ($CH_2{=}C{=}CH_2$, MeOH, and EtOH) to react with hydroxide ions (HO^-), generated by electron impact ionization of a gas mixture of N_2O and CH_4. The $CH_2{=}C{=}\dot{C}^-$ anion was prepared by allowing O^-, generated by electron impact ionization of N_2O, to react with $CH_2{=}C{=}CH_2$, forming $CH_2{=}C{=}\dot{C}^-$ and H_2O. As discussed below, we assume that only the $CH_2{=}C{=}\dot{C}^-$ anion is present without contamination by the isomeric propargylene ion ($H\dot{C}{=}C{=}CH^-$). The 1-propynyl anion ($CH_3C{\equiv}C^-$) was prepared by allowing F^-, formed by electron impact ionization of NF_3, to react with the commercially available trimethylsilyl derivative (TMS) of methylacetylene, $CH_3C{\equiv}C$-TMS.[34] This method of preparation assures that only the desired 1-propynyl anion is formed and not the isomeric allenyl anion ($CH_2{=}C{=}CH^-$). Each of these ions was mass-selected by a quadrupole mass filter, injected into the reaction flow tube (with helium pressures about 0.50 Torr) and, after reaching thermal equilibrium with the bath gas, allowed to react with selected neutral reagents. Ion products were monitored using a second quadrupole mass filter and electron multiplier. Ion−molecule rate coefficients were determined by plotting the parent ion signal intensity (ion counts s^{-1}) against the reaction distance (which is related to reaction time) for a measured neutral flow. Neutral reagent flows were determined from the pressure change as a function of time in a calibrated volume system. Product branching ratios were determined by plotting the fractional abundance of each product ion versus the extent of reaction (defined as the ratio of product ion signal to total ion signal at each reaction distance). The plot was extrapolated to zero reaction distance to eliminate the effects of differential diffusive loss of ions and possible secondary reactions. Corrections for the mass discrimination of the detection system were made in the reaction between the ethoxide anion and allene, where a small amount of adduct was observed in addition to the allenyl anion. The reported rate coefficients and branching ratios are the average values of at least three determinations, unless otherwise indicated; error bars represent one standard deviation of the mean of these measurements. The absolute accuracy of these measurements is estimated to be ±20%.

C. The Gas-Phase Acidity of Allene. We report selected literature values for ΔG_f, ΔH_f, ΔG_{acid}, and ΔH_{acid} of allene and related compounds in Table 1.[23,30,35-37] The gas-phase enthalpy of deprotonation of allene ($\Delta H_{acid} = 380.7 \pm 1.2$ kcal mol^{-1}) was obtained from the thermochemical cycle in eqs 1−4 using the experimentally determined electron affinity for the propargyl radical ($CH_2{=}C{=}\dot{C}H$), the ionization potential of hydrogen, and the calculated bond dissociation energy for $CH_2{=}C{=}CH{-}H$.[23a] $\Delta G_{acid}(CH_2{=}C{=}CH_2)$ was derived from $\Delta H_{acid}(CH_2{=}C{=}CH_2)$ using $\Delta S_{acid}(CH_2{=}C{=}CH_2) = 28.0 \pm 0.5$ cal mol^{-1} K^{-1} (see eq 19). To our knowledge this work represents the first attempt to measure the gas-phase acidity of allene directly.[23b] In Table 2 we report the theoretical value for $\Delta H_{acid}(CH_2{=}C{=}CH_2)$ determined from *ab initio* Gaussian-2 ("G2") calculations[38,39] using Gaussian 92.[40] The result ($\Delta H_{acid,298K}(CH_2{=}C{=}CH_2) = 382.4$ kcal mol^{-1}) is in good agreement with the literature value reported in Table 1. The optimized *ab initio* geometry of the allenyl anion using Gaussian 92[40] (MP2(FU)/6-311+G**//MP2(FU)/6-311+G**) is shown in Figure 5. In accord with

(26) Bartmess, J. E.; Scott, J. A.; McIver, R. T., Jr. *J. Am. Chem. Soc.* **1979**, *101*, 6046−6056.
(27) Lias, S. G.; Shold, D. M.; Ausloos, P. *J. Am. Chem. Soc.* **1980**, *102*, 2540.
(28) Bierbaum, V. M.; Schmitt, R. J.; DePuy, C. H.; Mead, R. H.; Schulz, P. A.; Lineberger, W. C. *J. Am. Chem. Soc.* **1981**, *103*, 6262.
(29) Oakes, J. M.; Jones, M. E.; Bierbaum, V. M.; Ellison, G. B. *J. Phys. Chem.* **1983**, *87*, 4810.
(30) Meot-Ner (Mautner), M.; Sieck, L. W. *J. Phys. Chem.* **1986**, *90*, 6687−6690.
(31) Damrauer, R.; Krempp, M.; O'Hair, R. A. J.; Simon, R. A. *Int. J. Mass Spectrom. Ion Proc.* **1992**, *117*, 199−211.
(32) Kebarle, P. *J. Am. Soc. Mass Spectrom.* **1992**, *3*, 1.
(33) Van Doren, J. M.; Barlow, S. E.; DePuy, C. H.; Bierbaum, V. M. *Int. J. Mass Spectrom. Ion Proc.* **1987**, *81*, 85.
(34) DePuy, C. H.; Bierbaum, V. M.; Flippin, L. A.; Grabowski, J. J.; King, G. K.; Schmitt, R. J. *J. Am. Chem. Soc.* **1979**, *101*, 6443.
(35) Lias, S. G.; Bartmess, J. E.; Liebman, J. F.; Holmes, J. L.; Levin, R. D.; Mallard W. G. *J. Phys. Chem. Ref. Data* **1988**, *17*, Suppl. No. 1, with updates from NIST negative ion energetics database (V. 2.07) and NIST standard reference database 19A (V. 1.1).
(36) Rosenstock, H. M.; Draxl, K.; Steiner, B. W.; Herron, J. T. *J. Phys. Chem. Ref. Data* **1977**, Suppl. 6.
(37) Stull, D. R.; Westrum, E. F., Jr.; Sinke, G. C. *The Chemical Thermodynamics of Organic Compounds*; John Wiley & Sons, Inc.: New York, 1969.
(38) Curtiss, L. A.; Raghavachari, K.; Trucks, G. W.; Pople, J. A. *J. Chem. Phys.* **1991**, *94*, 7221.
(39) Smith, B. J.; Radom, L. *J. Phys. Chem.* **1991**, *95*, 10549−10551.

Table 1. Selected Literature Values[a] for Gas-Phase Acidities and Heats of Formation (kcal mol^{-1}) (All Values Are at 298 K)

compd (RH)	ΔG_f(RH)	ΔH_f(RH)	$\Delta H_f(R^-)$[b]	ΔG_{acid} (RH)	ΔH_{acid} (RH)
CH_2=C=CH−H	48.37[c]	45.92[c]	60.9	372.4 ± 1.2[d]	380.7 ± 1.2[e]
H-CH_2C≡CH	46.47[c]	44.32[c]	60.9	374.3 ± 1.2[f]	382.3 ± 1.2[e]
CH_3C≡C−H	46.47[c]	44.32[c]	59.7	373.4 ± 2.4[g]	381.1 ± 2.1[h]
CH_3O−H		−48.2 ± 0.1	−32.3 ± 0.1	375.0 ± 0.7[i]	381.6 ± 0.7[j]
CH_3CH_2O−H		−56 ± 0.1	−43.3 ± 0.1	371.9 ± 0.8[i]	378.5 ± 0.8[j]

[a] Reference 35 unless otherwise indicated. Error bars are included whenever they are specified in the source reference. [b] Calculated from $\Delta H_f(R^-) = \Delta H_f(RH) + \Delta H_{acid}(RH) - \Delta H_f(H^+)$ using values in Table 1 and $\Delta H_f(H^+) = 365.7$ kcal mol^{-1} (ref 35). [c] References 36 and 37. Also see ref 51. [d] Calculated from $\Delta G_{acid}(RH) = \Delta H_{acid}(RH) - T\Delta S_{acid}(RH)$ using $\Delta H_{acid}(CH_2$=C=CH−H) in Table 1 and $\Delta S_{acid}(CH_2$=C=CH−H) = 28.0 ± 0.5 cal mol^{-1} K^{-1} (eq 19). [e] Reference 23. [f] Calculated from ΔG_{acid}(H−CH_2C≡CH) = $\Delta G_{acid}(CH_2$=C=CH−H) + $\Delta G_f(CH_2$=C=CH_2) − $\Delta G_f(CH_3$C≡CH) (eq 23) and the values in Table 1. [g] Calculated from $\Delta G_{acid}(RH) = \Delta H_{acid}(RH) - T\Delta S_{acid}(RH)$ using $\Delta H_{acid}(CH_3$C≡C−H) in Table 1 and $\Delta S_{acid}(CH_3$C≡C−H) = 26.0 ± 1.4 cal mol^{-1} K^{-1} (ref 35). [h] Reference 35 but see ref 50. [i] From $\Delta G_{acid}(RH) = \Delta H_{acid}(RH) - T\Delta S_{acid}(RH)$, using $\Delta H_{acid}(RH)$ in Table 1 (ref 30) and $\Delta S_{acid}(CH_3OH)$ = 22.0 ± 0.5 cal mol^{-1} K^{-1} and $\Delta S_{acid}(CH_3CH_2OH)$ = 22.0 ± 1.1 cal mol^{-1} K^{-1} (ref 35). [j] Reference 30.

Table 2. Theoretical Gas-Phase Acidities[a] in kcal mol^{-1} (Error Bars Are Estimated To Be ±2 kcal mol^{-1})

	ΔH_{acid}(RH)	
RH	0 K	298 K[b]
CH_2=C=CH−H	381.5	382.4
H-CH_2C≡CH	382.3	383.2
CH_3C≡C−H	381.3	382.1

[a] G2 calculations (refs 38 and 39) were performed using Gaussian 92 (ref 40). ZPE were scaled by 0.8929. Calculations were performed using a software program written by Ochterski, J. Personal communication, 1993. [b] 0 K energies were converted to 298 K by standard methods (ref 53) using a software program written by Rablen, P. Personal communication, 1993. Anion frequencies less than 1000 cm^{-1} were treated as vibrations rather than hindered rotations. This approximation is not expected to affect ΔH_{acid}(298K) for CH_2=C=CH−H and H−CH_2C≡CH, given the conjugated structure of the anion (**1**); however, it may affect ΔH_{acid}(298 K) for CH_3C≡C−H since the anion contains a methyl rotor.

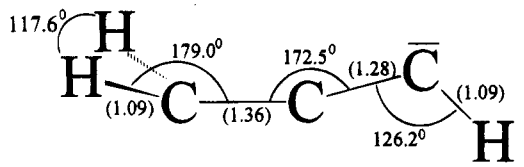

1

Figure 5. Optimized geometry for the $C_3H_3^-$ anion at the MP2(FU)/6-311+G** level of theory using Gaussian 92 (ref 40). Bond lengths (in parentheses) are in Angstroms.

previous theoretical[41,42] and experimental[23,43] results, we find that the geometry of this anion more closely resembles the allenyl anion (CH_2=C=CH^-) than the propargyl anion ($^-CH_2$C≡CH), hence we will refer to it as CH_2=C=CH^- or **1**.

Both the experimental and theoretical values reported in Tables 1 and 2 suggest that ΔH_{acid}(allene) equals roughly 381 kcal mol^{-1}. Using ΔS_{acid} = 28.0 ± 0.5 cal mol^{-1} K^{-1} (eq 19), this corresponds to ΔG_{acid}(allene) = 373 kcal mol^{-1}. This places allene intermediate between methanol (ΔG_{acid} = 375.0 ± 0.7 kcal mol^{-1}) and ethanol (ΔG_{acid} = 371.9 ± 0.8 kcal mol^{-1}), also reported in Table 1. We therefore selected these two alcohols as our reference acids. In principle, after the reference acid(s) have been selected, the rate coefficients for the forward (k_8 and k_9) and reverse proton transfer reactions

Scheme 1

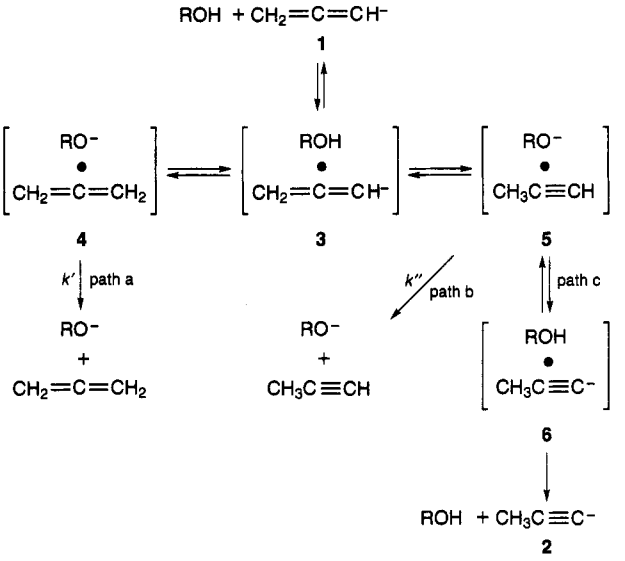

(k_{-8} and k_{-9}) can be determined:

$$MeO^- + CH_2{=}C{=}CH_2 \underset{k_{-8}}{\overset{k_8}{\rightleftharpoons}} CH_2CCH^- + MeOH \quad (8)$$

$$EtO^- + CH_2{=}C{=}CH_2 \underset{k_{-9}}{\overset{k_9}{\rightleftharpoons}} CH_2CCH^- + EtOH \quad (9)$$

As we will show, however, these measurements are more complicated than they first appear. The first difficulty arises as a result of the ambiguity in the protonation site of the allenyl anion (**1**). As illustrated in Scheme 1, protonation of **1** can take place within the ion−molecule complex (**3**) to form either allene (**4**) or methylacetylene (**5**). Reaction products RO^- and CH_2=C=CH_2 are formed with a rate coefficient k' while reaction products RO^- and CH_3C≡CH are formed with a rate coefficient k''. Note that both pathways produce the same product ion (RO^-). As a result, in our instrument we measure the sum of these processes, that is, $k_{exp} = k' + k''$. To determine the gas-phase acidity of allene, however, we must isolate k' from k_{exp}, which corresponds to k_{-8} for ROH = MeOH and k_{-9} for ROH = EtOH. Since k' cannot be measured experimentally, we estimate its value using equilibrium thermodynamics. The ratio of the fractional abundance of methylacetylene ([CH_3C≡CH]) to allene ([CH_2=C=CH_2]) formed in Scheme 1 can be estimated from the room temperature (298 K) equilibrium constant (K_{eq}) for isomerization of allene to methylacetylene (eq 10).[44] K_{eq} (eq 11) can be calculated from the relationship $\delta\Delta G_f = -RT \ln K_{eq} = -1.9$ kcal mol^{-1} where we used the

(40) Frisch, M. J.; Trucks, G. W.; Head-Gordon, M.; Gill, P. M. W.; Wong, M. W.; Foresman, J. B.; Johnson, B. G.; Schlegel, H. B.; Robb, M. A.; Replogle, E. S.; Gomperts, R.; Andres, J. L.; Raghavachari, K.; Binkley, J. S.; Gonzalez, C.; Martin, R. L.; Fox, D. J.; Defrees, D. J.; Baker, J.; Stewart, J. J. P.; Pople, J. A. *Gaussian 92, Revision C*; *Gaussian, Inc.*: Pittsburgh, PA, 1992.

(41) Wilmshurt, J. K.; Dykstra, C. E. *J. Am. Chem. Soc.* **1980**, *102*, 4668−4672.

(42) Li, W.-K. *Croat. Chem. Acta* **1988**, *61*, 833−842.

(43) van Dongen, J. P. C. M.; van Dijkman, H. W. D.; de Bie, M. J. A. *Recl. Trav. Chim. Pays-Bas* **1974**, *93*, 29.

values of ΔG_f given in Table 1 to obtain $\delta\Delta G_f$.

$$CH_2{=}C{=}CH_2 \overset{K_{eq}}{\rightleftharpoons} CH_3C{\equiv}CH \qquad (10)$$

$$K_{eq} = \frac{[CH_3C{\equiv}CH]}{[CH_2{=}C{=}CH_2]} = 24.74 \qquad (11)$$

Since paths a and b are the only two channels that lead to the formation of RO^-, then $[CH_2{=}C{=}CH_2] + [CH_3C{\equiv}CH] = 1$ and we can solve for the absolute fractional abundances. We find that $[CH_2{=}C{=}CH_2] = 0.039$ and $[CH_3C{\equiv}CH] = 0.961$. Hence, k_{-8} and k_{-9} will correspond to $0.039(k_{exp})$ for the k_{exp} measured in the reactions with MeOH and EtOH, respectively.

A second complication that can interfere with the determination of k_{-8} and k_{-9} arises from the possibility of isomerization within the ion–molecule complex, also illustrated in Scheme 1. In addition to reaction paths a and b, it is also possible for RO^- to abstract the terminal proton from methylacetylene (path c) and form $CH_3C{\equiv}C^-$ with ROH (**6**). If complex **6** separates, ROH and $CH_3C{\equiv}C^-$ (**2**) are formed, and the net reaction is isomerization of the allenyl anion (**1**) to the lower energy methylacetylenyl anion (**2**). The difference between the heats of formation of the two anions (Table 1) predicts that isomerization is exothermic by 1.2 kcal mol^{-1}. As a result, isomerization is the thermodynamically favored pathway in the methanol reaction. Based on the appropriate differences in ion and neutral heats of formation reported in Table 1, path a in the methanol reaction is endothermic by 0.9 kcal mol^{-1} and path b is exothermic by 0.7 kcal mol^{-1}. In contrast, isomerization is the least exothermic pathway in the ethanol reaction where paths a and b are predicted to be exothermic by 2.2 and 3.8 kcal mol^{-1}, respectively.

An isomerization pathway can yield spurious values for k_{-8} and k_{-9} since it leads to the formation of a product ion with the same mass-to-charge ratio as the parent ion. If the concentration of this product ion is allowed to build up, one can inadvertently measure a rate coefficient for a mixture of ions. For this reason, we devised several tests to evaluate the importance of isomerization in the $CH_2{=}C{=}CH^-$ (**1**) + ROH proton transfer reactions. We first used chemical reactivity with CS_2 to probe for isomerization of **1** to **2**. Previous investigations in our laboratory[45] have shown that **1** reacts with CS_2 to produce three products (eq 12). In this work, we establish that **2** reacts with CS_2 to product two products, a sulfur abstraction product at *m/z* 71 and the adduct ion at *m/z* 115 (eq 13):

	m/z		
CH_2CCH^- + CS_2 (**1**)	57	$HCCS^-$ + $CH_2{=}C{=}S$	(12)
	81	C_4HS^- + H_2S	
	115	$C_4H_3S_2^-$	
CH_3CC^- + CS_2 (**2**)	71	$C_3H_3S^-$ + CS	(13)
	115	$C_4H_3S_2^-$	

Note that the *m/z* 71 ion is formed only by the $CH_3C{\equiv}C^-$ isomer. We utilized this difference in reactivity between the two isomers to probe for the presence of **2**. HO^- and allene were allowed to react in the first flow tube. The resulting *m/z* 39 ions (**1**) were injected into the second flow tube and allowed to react with methanol (or ethanol), added at the injector. CS_2 was added further downstream, and the product ion spectrum was examined for the appearance of *m/z* 71. A small quantity of this ion was observed when methanol was the neutral reagent, indicating the presence of **2**. We repeated this experiment with ethanol as the neutral reagent, but in this case no *m/z* 71 ions were observed.

Scheme 2

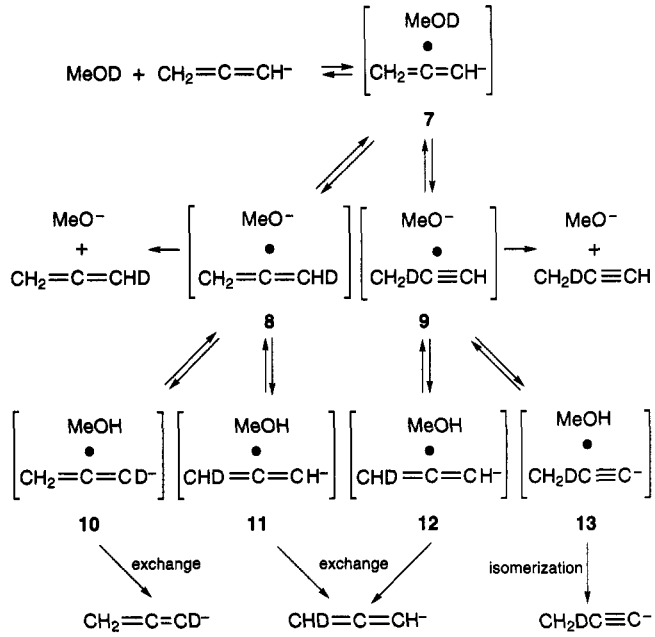

As a second test for isomerization we examined the H/D exchange reaction of $CH_2{=}C{=}CH^-$ with MeOD. In the absence of isomerization, H/D exchange is a thermoneutral process (assuming no isotope effects) and occurs by the mechanism illustrated in Scheme 2. After formation of the initial ion–molecule complex (**7**), deuteron transfer results in the formation of **8** or **9**, deuterium analogs of **4** and **5**. If **8** forms, the complex can of course separate to yield MeO^- as in the unlabeled reaction, but alternatively MeO^- can abstract a proton before escaping the ion–molecule complex and form **10** or **11**, which upon separation will yield the exchange products, $CH_2{=}C{=}CD^-$ or $CHD{=}C{=}CH^-$. Similarly if **9** forms, proton transfer will lead to the formation of **12** which upon separation will yield $CHD{=}C{=}CH^-$. In subsequent collisions with MeOD, the monodeuterated allenyl anion can continue to undergo analogous H/D exchange until ultimately $CD_2{=}C{=}CD^-$ is formed.

As in Scheme 1, there is also an isomerization pathway in Scheme 2. If **9** forms, MeO^- can abstract the terminal proton from methylacetylene to form **13** which upon separation will lead to the formation of $CH_2DC{\equiv}C^-$. (For simplicity we show only the most direct isomerization pathway but, for example, complex **10** can also undergo reverse reaction to form $[MeO^- \cdot CH_3C{\equiv}CD]$ from which $CH_3C{\equiv}C^-$ can be produced.) Unlike $CHD{=}C{=}CH^-$ and $CH_2{=}C{=}CD^-$, however, $CH_2DC{\equiv}C^-$ will not undergo further H/D exchange in subsequent collisions with MeOD since its carbanionic site contains no exchangeable hydrogens. To incorporate a second deuterium this ion must rearrange to a less energetically favorable isomer, $CHD{=}C{=}CD^-$, and as a result the exchange process becomes endothermic ($\Delta H_{rxn} = 1.2$ kcal mol^{-1}). Thus the H/D exchange rate coefficient for the reaction of $CH_2DC{\equiv}C^-$ + MeOD should be quite small and the H/D exchange rate of $CH_2{=}C{=}CH^-$ should slow down considerably if ever the $CH_2DC{\equiv}C^-$ ion is formed. Our independent investigations of the reaction of $CH_3C{\equiv}C^-$ + MeOD support this conclusion. As shown in

(44) The room temperature equilibrium constant for the isomerization of allene to methylacetylene also should represent the ratio of methylacetylene to allene formed from the ion–molecule complex (**3**), assuming that the complex has reached thermal equilibrium.

(45) DePuy, C. H. *Org. Mass Spectrom.* **1985**, *20*, 556.

Table 3. Experimental Branching Ratios and Rate Coefficients (k, units 10^{-10} cm^3 molecule^{-1} s^{-1}) for Deuterium-Labeled Reactions

reactants		branching ratios	products	rate coefficients k_{exp}	k_{coll}[a]	efficiency (k_{exp}/k_{coll})
CH_2=C=CH^- + MeOD	→	0.60	MeO^- + C_3H_3D	11 ± 1	17.9	0.61
	→	0.40[b]	$C_3H_2D^-$ + MeOH			
CH_2=C=CH^- + EtOD	→	0.93	EtO^- + C_3H_3D	19[c]	17.9	1.1
	→	0.07[b]	$C_3H_2D^-$ + EtOH			
$CH_3C{\equiv}C^-$ + MeOD[d]	→	≥0.97	MeO^- + $CH_3C{\equiv}CD$			
	→	≤0.03	CH_2CCD^- + MeOH			
$CH_3C{\equiv}C^-$ + EtOD	→	1.00	EtO^- + $CH_3C{\equiv}CD$			

[a] Collision rate calculated by average dipole orientation (ADO) theory (ref 47). [b] The branching ratio includes $C_3H_2D^-$ products formed by H/D exchange (e.g., CH_2=C=CD^-) and isomerization ($CH_2DC{\equiv}C^-$). Model calculations (see text) suggest that the branching ratio for H/D exchange without isomerization is 0.36 in the MeOD reaction and 0.02 in the EtOD reaction. [c] Average of two measurements; agreement is ±2%. [d] Fractional abundances were estimated from the product ion spectrum.

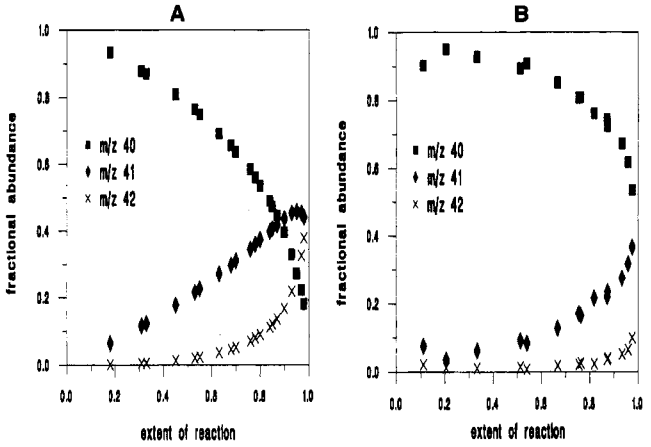

Figure 6. Comparison of model and experimental data in the H/D exchange reaction of CH_2=C=CH^- with MeOD. In part A we model the expected fractional abundances of the monodeuterated (m/z 40), dideuterated (m/z 41), and trideuterated (m/z 42) product analogs of CH_2=C=CH^- (**1**) versus extent of reaction assuming no isomerization takes place. In part B we plot the experimental data. Discrepancies with part A suggest that isomerization does take place.

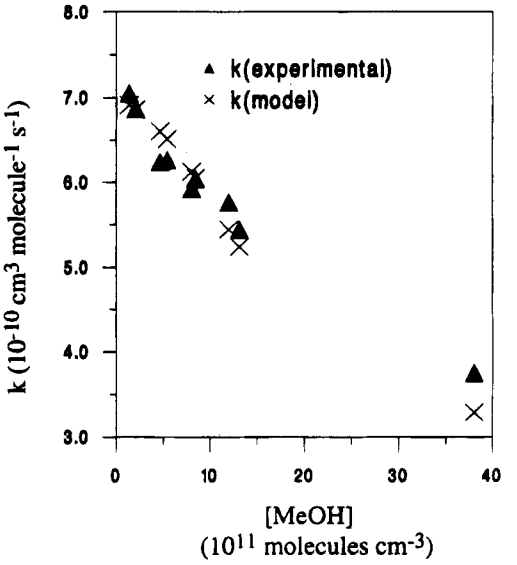

Figure 7. The solid triangles represent the experimentally observed rate coefficients as a function of increasing [MeOH] for the reaction of CH_2=C=CH^- (m/z 39) + MeOH. The "×"s represent a model of the experimental data. The model includes $CH_3C{\equiv}C^-$ in addition to CH_2=C=CH^- for m/z 39 and assumes that $CH_3C{\equiv}C^-$ is formed in the course of the reaction via isomerization of CH_2=C=CH^-. In both the experimental and model data, significant decreases are observed in the rate coefficients as the MeOH concentration is increased.

Table 3, only a small amount of the exchange product (m/z 40) was detected (less than 3% of the total ion signal) when large quantities of MeOD were present, indicative of a slow and inefficient exchange process.

In light of the above arguments, we should observe a decrease in the consecutive H/D exchange rates of CH_2=C=CH^- with excess MeOD if isomerization takes place. The first H/D exchange should be the fastest since it reflects thermoneutral exchange and exothermic isomerization (Scheme 2). If $CH_2DC{\equiv}C^-$ is formed, however, subsequent H/D exchange rates should decline. The rate coefficient for the first H/D exchange can be determined from the data in Table 3. We monitored the disappearance of CH_2=C=CH^- in the presence of MeOD to determine the overall rate coefficient for the reaction. We simultaneously monitored the appearance of the products MeO^- and $C_3H_2D^-$ to determine their respective branching ratios. The appropriate branching ratio multiplied by the overall rate coefficient gives the desired quantity. We find that the rate coefficient for the formation of $C_3H_2D^-$ (which includes any isomerization that may have occurred) is 4.4 (±0.9) × 10^{-10} cm^3 molecule^{-1} s^{-1}.

We used this rate coefficient to construct the model shown in Figure 6A. We have plotted the fractional abundances of CHD=C=CH^- and CH_2=C=CD^- (m/z 40), CHD=C=CD^- and CD_2=C=CH^- (m/z 41), and CD_2=C=CD^- (m/z 42) which are expected versus the extent of reaction with MeOD, if the second and third H/D exchanges occur at the same rate as the first exchange, modified accordingly to reflect the changing number of exchangeable hydrogens. For example, in the first exchange [$CH_3O^- \cdot C_3H_3D$] is formed, hence CH_3OH can be formed in three ways. But in the second exchange [$CH_3O^- \cdot C_3H_2D_2$] is formed, and as a result CH_3OH can be formed in only two ways. Hence the rate coefficient for the second exchange is two-thirds that of the first exchange or 2.9 × 10^{-10} cm^3 molecule^{-1} s^{-1}. Analogously, the rate coefficient for the third exchange was estimated to be 1/3 that of the first exchange or 1.5 × 10^{-10} cm^3 molecule^{-1} s^{-1}.

The experimental data are plotted in Figure 6B, showing the observed fractional abundances of m/z 40, 41, and 42 versus the extent of reaction with MeOD. These data show significant deviation from the model in Figure 6A. In particular, the decay of m/z 40 is less steep in the experimental data (roughly a 40% drop in signal) as compared to the model, which predicts that the decline should be closer to 70%. As a result, m/z 41 and 42 rise less quickly than predicted. Once again, this evidence supports the presence of an isomerization pathway in the methanol reaction, although the observance of a small amount of fully deuterated $C_3D_3^-$ ions (m/z 42) suggests that some fraction of the allenyl anions survive without isomerization.

We did not analyze the corresponding reaction of CH_2=C=CH^- + EtOD, since in this case the branching ratio for H/D exchange (including isomerization) drops to 0.07 (Table 3). We attribute this drop to the increased acidity of ethanol

Table 4. Experimental Branching Ratios and Rate Coefficients (k, unit 10^{-10} cm^3 molecule^{-1} s^{-1})

reactants		branching ratios	products	rate coefficients k_{exp}[a]	k_{coll}[b]	efficiency (k_{exp}/k_{coll})
$CH_2{=}C{=}CH^-$ + MeOH[c]	→	1.00	MeO^- + C_3H_4	7.0[d]	18.0	0.39
$CH_2{=}C{=}CH^-$ + EtOH[c]	→	1.00	EtO^- + C_3H_4	16[e]	18.0	0.89
MeO^- + $CH_2{=}C{=}CH_2$	→	1.00	$C_3H_3^-$ + MeOH	9.4 ± 0.7	13.2	0.71
EtO^- + $CH_2{=}C{=}CH_2$	→	0.96	$C_3H_3^-$ + EtOH	0.18 ± 0.01	11.9	0.02
	→	0.04	$EtO^-C_3H_4$ (adduct)			
$CH_3C{\equiv}C^-$ + MeOH	→	1.00	MeO^- + $CH_3C{\equiv}CH$	2.9 ± 0.3	18.0	0.16
$CH_3C{\equiv}C^-$ + EtOH	→	1.00	EtO^- + $CH_3C{\equiv}CH$	14 ± 1	18.0	0.78

[a] Error bars represent one standard deviation of the mean of three or more measurements unless otherwise indicated. [b] Collision rate calculated by average dipole orientation (ADO) theory (ref 47). [c] The branching ratio and rate coefficient (k_{exp}) do not include the isomerization channel to form $CH_3C{\equiv}C^-$ since it cannot be detected in our instrument. Model calculations (see text) predict that the rate coefficient for isomerization is 3.5 × 10^{-11} cm^3 molecule^{-1} s^{-1} in the MeOH reaction and 1.0 × 10^{-10} cm^3 molecule^{-1} s^{-1} in the EtOH reaction. [d] Average of two measurements at low methanol concentrations to prevent contamination by $CH_3C{\equiv}C^-$; agreement was ±2%. Determinations (≥4) at higher concentrations are consistent with this value. [e] Result of one measurement at low ethanol concentration to prevent contamination by $CH_3C{\equiv}C^-$. Determinations (≥4) at higher concentrations are consistent with this value.

which decreases the probability of exchange in favor of proton transfer to form EtO^-. A tiny fraction of the $C_3HD_2^-$ species was detected after multiple collisons with EtOD, but incorporation of three deuteriums was not observed. Note that the branching ratio for exchange (0.07) also represents an upper limit on the fractional amount of allenyl anions that can undergo isomerization in the ethanol reaction.

The final and most quantitative evidence for isomerization of **1** to **2** appears in the rate coefficients for the undeuterated reactions of $CH_2{=}C{=}CH^-$ with MeOH or EtOH. In Figure 7 we plot the experimentally observed rate coefficient (k_{exp}) versus increasing MeOH concentration. Note the significant decrease in the apparent rate coefficient as [MeOH] increases. In the FA-SIFT apparatus ion–molecule reactions obey pseudo-first-order reaction kinetics since neutral concentrations (≈10^{12} molecules cm^{-3}) are typically eight orders of magnitude greater than ion concentrations (≈10^4 ions cm^{-3}). Hence, rate coefficients do not change with neutral concentration unless a mixture of isomeric ions is present. Indeed, such changes are often used to show that a mixture of isomeric ions is injected into the reaction flow tube. In this case, however, we believe that only **1** is injected into the second flow tube and that isomerization to **2** takes place in the course of the reaction with MeOH. We summarize the reaction steps in eqs 14 and 15 below:

$$\underset{\mathbf{1}}{CH_2{=}C{=}CH^-} + MeOH \xrightarrow{k_{14a}} MeO^- + CH_2{=}C{=}CH_2 \quad (14a)$$

$$\xrightarrow{k_{14b}} MeO^- + CH_3C{\equiv}CH \quad (14b)$$

$$\xrightarrow{k_{14c}} \underset{\mathbf{2}}{CH_3C{\equiv}C^-} + MeOH \quad (14c)$$

$$\underset{\mathbf{2}}{CH_3C{\equiv}C^-} + MeOH \xrightarrow{k_{15}} MeO^- + CH_3C{\equiv}CH \quad (15)$$

The isomeric ion **2** is formed in a primary reaction shown in eq 14c. It then goes on to react with MeOH in a secondary reaction (eq 15) to produce MeO^-, the same product ion that is formed by **1** (eqs 14a and 14b) but at a different rate. At low MeOH concentrations, the secondary reaction (eq 15) is unimportant. Any $CH_3C{\equiv}C^-$ ions that form by eq 14c have insufficient time in the flow tube to undergo a reactive collision with MeOH, hence the measured rate coefficient is that of the allenyl anion (**1**) with methanol. As the methanol concentration is increased, however, eq 15 becomes significant. As a result, the experimental rate coefficient reflects the combined loss of **1** and **2** with MeOH. Since the rate coefficient was observed to decrease as the methanol concentration was increased, the rate coefficient for **2** must be smaller than it is for **1**. Our independent measurements of the rate coefficient for the reaction of **2** with MeOH prove this to be the case (see below and Table 4).

To determine the gas-phase acidity of allene accurately, we must measure the rate coefficient for eq 14 with negligible contribution by eq 15. To achieve this goal, we used very low concentrations of MeOH. Indeed, we estimate that fewer than two collisions were allowed to take place between **1** and MeOH in the reaction flow tube. We report the result (7.0 × 10^{-10} cm^3 molecule^{-1} s^{-1}) in Table 4. This rate coefficient was determined by monitoring the disappearance of $CH_2{=}C{=}CH^-$ which is equivalent to the rate of formation of MeO^-, hence it equals the sum $k_{14a} + k_{14b}$.

We are unable to measure the rate coefficient for isomerization (k_{14c}) in our instrument; however, k_{14c} can be deduced mathematically by solving simultaneously[46] for the time-dependent concentrations of $CH_2{=}C{=}CH^-$ and $CH_3C{\equiv}C^-$ (derived from eqs 14 and 15):

$$\frac{d[CH_2{=}C{=}CH^-]}{dt} = -(k_{14a} + k_{14b} + k_{14c})[CH_2{=}C{=}CH^-][MeOH] \quad (16)$$

$$\frac{d[CH_3C{\equiv}C^-]}{dt} = k_{14c}[CH_2{=}C{=}CH^-][MeOH] - k_{15}[CH_3C{\equiv}C^-][MeOH] \quad (17)$$

The solutions to eqs 16 and 17 can be used to solve for d ln[$CH_2{=}C{=}CH^-$ + $CH_3C{\equiv}C^-$]/dt which in turn can be used to reproduce our experimentally determined rate coefficients (k_{exp}):

$$k_{exp} = -\frac{d\ln([CH_2{=}C{=}CH^-] + [CH_3C{\equiv}C^-])/dt}{[MeOH]} \quad (18)$$

All of the quantities in eqs 16–18 are known experimentally except k_{14c}. We know the initial concentrations of $CH_2{=}C{=}CH^-$ and $CH_3C{\equiv}C^-$, the concentration of MeOH (assumed to be constant since we operate under pseudo-first-order reaction conditions), the sum $k_{14a} + k_{14b}$ (Table 4), and k_{15} (Table 4). Hence, the unknown value k_{14c} can be determined iteratively; various values can be tried until good agreement between the calculated rate coefficient and the experimental rate coefficient

(46) Differential equations were solved using *Mathematica* (version 2.2) on a AIX Unix based IBM RISC 6000 system.

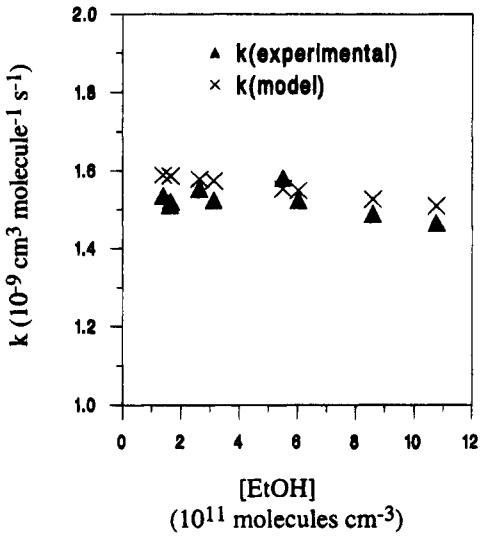

Figure 8. The solid triangles represent the experimentally observed rate coefficients as a function of increasing [EtOH] for the reaction of $CH_2{=}C{=}CH^-$ (m/z 39) + EtOH. The "×"s represent a model of the experimental data. The model includes $CH_3C{\equiv}C^-$ in addition to $CH_2{=}C{=}CH^-$ for m/z 39 and assumes that $CH_3C{\equiv}C^-$ is formed in the course of the reaction via isomerization of $CH_2{=}C{=}CH^-$. In both the experimental and model data, small decreases are observed in the rate coefficients as the EtOH concentration is increased.

is obtained over a wide range of methanol concentrations. The results are shown in Figure 7. Good agreement between the model and the experimental data is obtained when $k_{14c} = 3.5 \times 10^{-11}$ cm^3 molecule^{-1} s^{-1}. Assuming that the collision rate coefficient[47] for the $CH_2{=}C{=}CH^-$ + MeOH reaction is 1.8×10^{-9} cm^3 molecule^{-1} s^{-1} (Table 4), this corresponds to a reaction efficiency of 0.05.

The rate coefficient for isomerization (k_{14c}) allows us to interpret the rate coefficient for the reaction between **1** and MeOD. As discussed above, we used the labeled reaction to measure the overall rate coefficient ($k_{exp} = 1.1 (\pm 0.1) \times 10^{-9}$ cm^3 molecule^{-1} s^{-1}) and the branching ratio for H/D exchange (0.40) (Table 3). The product of these two gives 4.4 (± 0.9) $\times 10^{-10}$ cm^3 molecule $^{-1}$ s^{-1}, a value which includes the rate coefficients for both H/D exchange (forming e.g., $CH_2{=}C{=}CD^-$) and isomerization (forming $CH_2DC{\equiv}C^-$). If we subtract the proposed isomerization rate coefficient (3.5×10^{-11} cm^3 molecule^{-1} s^{-1}) from this sum, we obtain 4.0×10^{-10} cm^3 molecule^{-1} s^{-1}, the rate coefficient for exchange without isomerization. This value corresponds to a branching ratio for H/D exchange of 0.36 and a branching ratio for isomerization of 0.04.

The reaction between $CH_2{=}C{=}CH^-$ and EtOH can be analyzed in the same way as the MeOH reaction. In Figure 8 we plot the apparent rate coefficients measured for this reaction as a function of increasing ethanol concentration. Again a decrease is observed, but it is smaller in magnitude than the corresponding decrease observed in the methanol reaction (Figure 7). This finding is consistent with the results of the labeled study (Table 3) which suggest that 93% of $CH_2{=}C{=}CH^-$ ions react rapidly with EtOH to produce EtO^-, hence a build up of $CH_3C{\equiv}C^-$ ions does not occur. A set of equations analogous to eqs 14 and 15 can be written for the reaction of $CH_2{=}C{=}CH^-$ with ethanol. The experimentally determined rate coefficient for this reaction, corresponding to $k_{14a} + k_{14b}$, is reported in Table 4. We again used low concentrations of EtOH to make this measurement and obtained 1.6×10^{-9} cm^3 molecule^{-1} s^{-1}. Using equations analogous to eqs 16–18, we compared calculated rate coefficients with experimental data in an iterative manner to arrive at a rate coefficient for isomerization (corresponding to k_{14c}). Good agreement is achieved with the value 1.0×10^{-10} cm^3 molecule^{-1} s^{-1} (Figure 8). This value corresponds to a reaction efficiency of 0.06 based on the collision rate reported in Table 4. It also gives further insight into the rate coefficient for H/D exchange in the reaction with EtOD. According to the data in Table 3, the rate coefficient for H/D exchange is 1.33×10^{-10} cm^3 molecule^{-1} s^{-1} with a branching ratio of 0.07; however, as described above, this value includes both H/D exchange and isomerization. If we subtract from this sum the calculated rate coefficient for isomerization (1.0×10^{-10} cm^3 molecule^{-1} s^{-1}), we find that only a small fraction of collisions (less than 2%) undergo H/D exchange.

(47) Su, T.; Bowers, M. T. *Int. J. Mass Spectrom. Ion Phys.* **1973**, *12*, 347.

Scheme 3

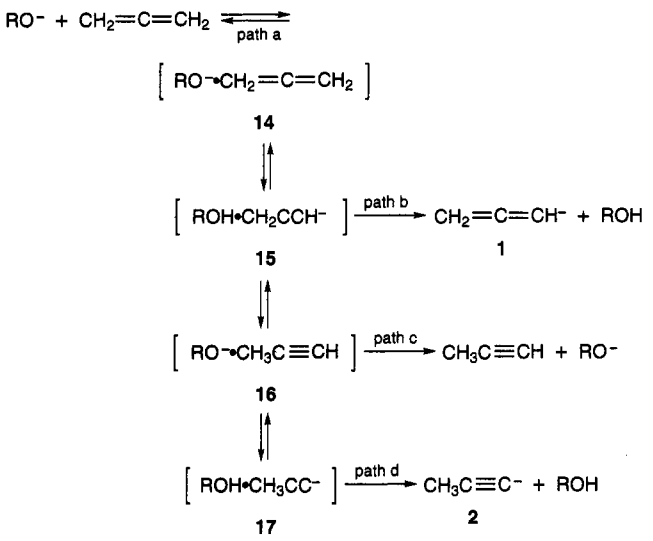

We now consider the forward reactions between MeO^- or EtO^- and allene. The rate coefficients were determined without complication (i.e., the rate coefficient did not vary with neutral concentration) and the results are reported in Table 4. While it was experimentally straightforward to measure these rate coefficients, interpretation of the data is again complicated by the possibility of isomerization. A possible mechanism is illustrated in Scheme 3, using RO^- to represent the methoxide and ethoxide ions. After formation of the initial ion–molecule complex (**14**), proton abstraction results in the formation of **15**. If **15** separates (path b), $CH_2{=}C{=}CH^-$ and ROH are formed. If ROH transfers a proton before separation however, **15** can form either **14** or **16**. Separation of **14** simply reforms the starting materials (path a), but separation of **16** (path c) forms the isomerized neutral, $CH_3C{\equiv}CH$, a pathway predicted to be exothermic by 1.6 kcal mol^{-1} (Table 1). Finally, as in Scheme 1, RO^- can abstract the terminal proton in methylacetylene to form **17** and ultimately **2**, the 1-propynyl anion with ROH (path d). According to the heats of formation given in Table 1, this pathway is exothermic when ROH is MeOH ($\Delta H_{rxn} = -2.1$ kcal mol^{-1}) and endothermic when ROH is EtOH ($\Delta H_{rxn} = 1.0$ kcal mol^{-1}). Unfortunately, it is difficult to evaluate experimentally the contributions of paths c and d. We cannot test for path c since the product ion formed has the same mass-to-charge ratio as the reactant ion. We did test for the presence of **2**, possibly formed by path d, using ion–molecule chemistry with CS_2 as described above, but with negative results.

The possible contribution by the competing pathways shown in Scheme 3 and the contribution by the competing pathways illustrated in Scheme 1 complicate the measurement of the gas-

Table 5. Rate Coefficients and $\delta\Delta G_{acid}$[a] for Proton Transfer Reactions

eq no.	k_{exp} (cm^3 molecule^{-1} s^{-1})	$\delta\Delta G_{acid}$ (kcal mol^{-1})
8	$MeO^- + CH_2{=}C{=}CH_2 \rightleftarrows CH_2{=}C{=}CH^- + MeOH$	−2.1
	$k_8 = 9.4 \pm 1.9 \times 10^{-10}$	
	$k_{-8} = 2.7 \pm 0.5 \times 10^{-11}$	
9	$EtO^- + CH_2{=}C{=}CH_2 \rightleftarrows CH_2{=}C{=}CH^- + EtOH$	0.77
	$k_9 = 1.7 \pm 0.3 \times 10^{-11}$	
	$k_{-9} = 6.2 \pm 1.2 \times 10^{-11}$	

[a] $\delta\Delta G_{acid} = \Delta G_{rxn} = -RT \ln K_{eq}$ where $K_{eq} = k_8/k_{-8}$ and k_9/k_{-9} for eqs 8 and 9, respectively. We use $R = 1.987$ cal mol^{-1} K^{-1} and $T = 298$ K. Errors for rate coefficients and for $\delta\Delta G_{acid}$ are estimated to be ±20%.

phase acidity of allene. Ideally, when using proton transfer kinetics to determine a gas-phase acidity, the desired protonation or deprotonation channel is the only pathway present. Whenever competing reaction channels are present, such as isomerization or adduct stabilization by a third body, a degree of ambiguity is introduced. Even when the branching ratio(s) for the competing channel(s) are known, to interpret these data one must make an assumption about the fate of those ions that followed the alternate path if this path had not been available. For these studies we assume that those ions would have decomposed to reactants rather than undergo proton transfer. With this assumption, a proton transfer rate coefficient measured in a reaction where a competing channel is present represents a lower limit to the ideal rate coefficient, the one that would be measured in the absence of the competing pathway(s). Thus, for example, in the forward reactions of $CH_2{=}C{=}CH^-$ with ROH we assume that the 5% of ions that underwent isomerization would have decomposed to reactants in the absence of the isomerization pathway. In the reverse direction, we assume that any ions that followed path c in Scheme 3 also would have decomposed to reactants rather than undergone proton transfer. Similarly, in the reaction with ethanol a small amount of adduct formation was observed. We again assume that these ions would have decomposed to reactants in the absence of a stabilizing collision with the buffer gas.[48]

With these limitations in mind, the gas-phase acidity of allene can be determined. Relevant data are summarized in Table 5. The forward rate coefficient k_8 is uncorrected, hence any contributions by competing pathways such as those illustrated in Scheme 3 are neglected. The forward rate coefficient k_9 is corrected for a small amount of adduct formation (4%) observed in the reaction (Table 4). The rate coefficients for the reverse reactions (k_{-8} and k_{-9}) are obtained by multiplying k_{exp} (determined at low neutral concentrations to prevent contamination by **2**) by 0.039, to partition the formation of $CH_2{=}C{=}CH_2$ relative to $CH_3C{\equiv}CH$ according to their room temperature equilibrium concentrations. In Table 5 we also report values for $\delta\Delta G_{acid}$ obtained from the ratio of the forward and reverse rate coefficients (K_{eq}) according to the relationship $\delta\Delta G_{acid} = \Delta G_{rxn} = -RT \ln K_{eq}$. We find that $\delta\Delta G_{acid}$ relative to methanol is −2.1 kcal mol^{-1} and that $\delta\Delta G_{acid}$ relative to ethanol is 0.77 kcal mol^{-1}. Errors are estimated to be less than ±20%. We converted the two relative gas-phase acidities to absolute gas-phase acidities using the relationship $\Delta G_{acid}(CH_2{=}C{=}CH_2) = \Delta G_{acid}(ROH) + \delta\Delta G_{acid}$, and we find that $\Delta G_{acid}(CH_2{=}C{=}CH_2) = 372.9$ kcal mol^{-1} when methanol is the reference alcohol and ΔG_{acid} $(CH_2{=}C{=}CH_2) = 372.7$ kcal mol^{-1} when ethanol is the reference alcohol. The two values are averaged and the absolute error is estimated to be ±3 kcal mol^{-1}. The final value, $\Delta G_{acid}(CH_2{=}C{=}CH_2) = 372.8 \pm 3$ kcal mol^{-1}, is reported in Table 6.

(48) The assigned error bars include uncertainties introduced by these assumptions.

Table 6. Final Experimental Gas-Phase Acidities (298 K)

compd	ΔG_{acid} (kcal mol^{-1})	ΔS_{acid} (cal mol^{-1} K^{-1})	ΔH_{acid} (kcal mol^{-1})
$CH_2{=}C{=}CH{-}H$	372.8 ± 3	28.0 ± 0.5[a]	381.1 ± 3
$H{-}CH_2C{\equiv}CH$[b]	374.7 ± 3		382.7 ± 3
$CH_3C{\equiv}C{-}H$	373.4 ± 2.3	26.0 ± 1.4[c]	381.1 ± 3
$CH_2{=}C{=}C{-}H$[d]	364 ± 5		372 ± 5

[a] From eq 19. [b] ΔG_{acid} and ΔH_{acid} for $H{-}CH_2C{\equiv}CH$ were calculated according to eqs 23 and 24 using $\delta\Delta G_f = 1.9$ kcal mol^{-1}, $\delta\Delta H_f = 1.6$ kcal mol^{-1}, and $\Delta H_{acid}(CH_2{=}C{=}CH_2) = 381.1 \pm 3$ kcal mol^{-1} (see Table 1, ref 51, and text). [c] Reference 35. [d] Both ΔG_{acid} and ΔH_{acid} were obtained by bracketing methods (see text and Table 7).

Reasonable agreement is observed between the difference in acidities of methanol and ethanol measured in this work, $\delta\Delta G_{acid} = 2.9$ kcal mol^{-1} (where we estimate the error to be 20% or ±0.6 kcal mol^{-1}), and that reported by Bartmess et al.,[26] $\delta\Delta G_{acid} = 3.1 \pm 0.2$ kcal mol^{-1}. This agreement is encouraging and suggests that although the various isomerization schemes discussed above may contribute to some degree, they do not significantly affect the final gas-phase acidity.

The gas-phase acidity was converted to ΔH_{acid} using the relationship $\Delta H_{acid} = \Delta G_{acid} + T\Delta S_{acid}$, yielding $\Delta H_{acid}(CH_2{=}C{=}CH_2) = 381.1 \pm 3$ kcal mol^{-1} (Table 6). $\Delta S_{acid}(CH_2{=}C{=}CH_2)$ was determined from the equation:

$$\Delta S_{acid}(CH_2{=}C{=}CH_2) = S(CH_2{=}C{=}CH^-) + S(H^+) - S(CH_2{=}C{=}CH_2) \quad (19)$$

using $S(CH_2{=}C{=}CH^-) = 60.24$ cal mol^{-1} K^{-1};[49] $S(H^+) = 26.04$ cal mol^{-1} K^{-1};[16] and $S(CH_2{=}C{=}CH_2) = 58.3$ cal mol^{-1} K^{-1}.[37] Uncertainties in $T\Delta S_{acid}$ are estimated to be no greater than 0.5 kcal mol^{-1}. The final result, $\Delta H_{acid}(CH_2{=}C{=}CH_2) = 381.1 \pm 3$ kcal mol^{-1}, is within error bars of both the experimental value reported in Table 1 (380.7 ± 1.2 kcal mol^{-1}) and the theoretical value reported in Table 2 (382.4 ± 2.0 kcal mol^{-1}).

D. The Gas-Phase Acidity of Methylacetylene. Literature values for ΔG_{acid} and ΔH_{acid} of methylacetylene ($CH_3C{\equiv}C{-}H$) are reported in Table 1 (see ref 50). The theoretical value for $\Delta H_{acid}(CH_3C{\equiv}C{-}H)$ is reported in Table 2. The *ab initio* calculation is in good agreement with the literature value, but it does reverse the order of $\Delta H_{acid}(CH_3C{\equiv}C{-}H)$ and $\Delta H_{acid}(CH_2{=}C{=}CH{-}H)$. We repeated the gas-phase acidity measurement for $CH_3C{\equiv}C{-}H$ using proton transfer kinetics and methanol and ethanol as our reference acids. We studied this reaction in one direction only, $CH_3C{\equiv}C^- + ROH$, using a trimethylsilyl derivative ($CH_3C{\equiv}C$-TMS) to prepare the

(49) The value for $S(CH_2{=}C{=}CH^-)$ was obtained using the output of a Gaussian 92 frequency calculation (UHF/6-31+G*) (ref 40). Zero-point energies were corrected by 0.8934. The entropy (S_{298}) was determined by standard methods (refs 16 and 53) using a software program developed by Rablen, P. Personal communication, 1993. All frequencies under 1000 cm^{-1} were treated as vibrations rather than hindered rotations. This approximation is reasonable given the allenyl-like structure of the anion (**1**).

(50) We use Lias et al. (ref 35) as the reference for $\Delta H_{acid}(CH_3C{\equiv}C{-}H)$, a value determined experimentally by Bartmess et al. (ref 26). Meot-Ner and Sieck (ref 30) recommend this value be increased to 382.0 kcal mol^{-1} based on a redetermination of the absolute acidity of methanol. While we agree with this change in principle (and report the corrected gas-phase acidities of methanol and ethanol in Table 1) we do not make it for $CH_3C{\equiv}C{-}H$ since we believe that the Bartmess et al. value may already be too large. It is likely that a mixture of isomers $CH_2{=}C{=}CH^-$ (**1**) and $CH_3C{\equiv}C^-$ (**2**) was present in their apparatus. Since $\Delta H_{acid}(H{-}CH_2C{\equiv}CH)$ is larger than $\Delta H_{acid}(CH_3C{\equiv}C{-}H)$ a mixture of isomers would tend to increase the value of ΔH_{acid} measured. Thus, by not correcting for the change in the absolute acidity scale, the two factors will tend to cancel.

$CH_3C{\equiv}C^-$ ion. The reverse direction ($RO^- + CH_3C{\equiv}CH$) was not studied since commercially available methylacetylene contains a significant acetylene impurity which reacts with both MeO^- and EtO^- in fast, exothermic proton transfer reactions. Moreover, methylacetylene has two non-equivalent hydrogens which are believed to differ in acidity by no more than 1.2 kcal mol^{-1} (Table 1). Thus both could be abstracted by the same base, making it difficult to isolate the rate coefficient for the abstraction of the acetylenic proton. We found the rate coefficients for the reactions $CH_3C{\equiv}C^-$ with MeOH and EtOH to be 2.9 ($\pm$0.3) $\times$ 10^{-10} and 1.4 ($\pm$0.1) $\times$ 10^{-9} cm^3 $molecule^{-1}$ s^{-1}, respectively, corresponding to reaction efficiencies of 0.16 and 0.78 (Table 4). By bracketing the gas-phase acidity of $CH_3C{\equiv}C{-}H$ between methanol (ΔG_{acid} = 375.0 $\pm$ 0.7 kcal mol^{-1}) and ethanol (ΔG_{acid} = 371.9 $\pm$ 0.8 kcal mol^{-1}), $\Delta G_{acid}(CH_3C{\equiv}C{-}H)$ was found to be 373.4 $\pm$ 2.3 kcal mol^{-1} (Table 6), where the error bars were chosen to reflect the maximum possible difference in acidities between the two reference acids. Using $\Delta S_{acid}(CH_3C{\equiv}C{-}H)$ = 26.0 $\pm$ 1.4 cal mol^{-1} K^{-1},[35] we find $\Delta H_{acid}(CH_3C{\equiv}C{-}H)$ = 381.1 $\pm$ 3 kcal mol^{-1} (Table 6). This value is in exact agreement with the literature value reported in Table 1 and in good agreement with the theoretical value reported in Table 2 (382.1 $\pm$ 2 kcal mol^{-1}).

Note that methylacetylene has two non-equivalent hydrogen atoms, each with a corresponding value of ΔG_{acid} and ΔH_{acid}. Abstraction of an acetylenic proton results in the formation of the 1-propynyl anion ($CH_3C{\equiv}C^-$), whereas abstraction of a methyl group proton results in the formation of $^-CH_2C{\equiv}CH$, a resonance structure of the allenyl anion:

$$^-CH_2C{\equiv}CH \leftrightarrow CH_2{=}C{=}CH^- \quad (20)$$

As a result, the gas-phase acidities of $H{-}CH_2C{\equiv}CH$ and $CH_2{=}C{=}CH{-}H$ are linked. By definition,[35] the gas-phase acidities of allene (eq 21) and methylacetylene (eq 22) are:

$$\Delta G_{acid}(CH_2{=}C{=}CH_2) = \Delta G_f(CH_2{=}C{=}CH^-) + \Delta G_f(H^+) - \Delta G_f(CH_2{=}C{=}CH_2) \quad (21)$$

$$\Delta G_{acid}(H{-}CH_2C{\equiv}CH) = \Delta G_f(CH_2{=}C{=}CH^-) + \Delta G_f(H^+) - \Delta G_f(CH_3C{\equiv}CH) \quad (22)$$

$$\Delta G_{acid}(CH_2{=}C{=}CH_2) - \Delta G_{acid}(H{-}CH_2C{\equiv}CH) = -[\Delta G_f(CH_2{=}C{=}CH_2) - \Delta G_f(CH_3C{\equiv}CH)] \quad (23)$$

Since each neutral dissociates to form the same ion, the difference in their gas-phase acidities will equal minus the difference in their free energies of formation (eq 23). The free energies of formation of allene and methylacetylene (Table 1) differ by 1.9 kcal mol^{-1}, hence the difference between the acidities of allene and methylacetylene ($H{-}CH_2C{\equiv}CH$) will also equal 1.9 kcal mol^{-1}. In Table 6 we report $\Delta G_{acid}(CH_2{=}C{=}CH_2)$ = 372.8 $\pm$ 3 kcal mol^{-1}, thus $\Delta G_{acid}(H{-}CH_2C{\equiv}CH)$ = 374.7 $\pm$ 3 kcal mol^{-1}, also reported in Table 6. This value is in good agreement with the literature value of $\Delta G_{acid}(H{-}CH_2C{\equiv}CH)$ reported in Table 1 (ΔG_{acid} = 374.3 $\pm$ 1.2 kcal mol^{-1}) which was derived from $\Delta G_{acid}(CH_2{=}C{=}CH_2)$ in an analogous manner.

The same relationship holds true for ΔH_{acid}, that is:

$$\Delta H_{acid}(CH_2{=}C{=}CH_2) - \Delta H_{acid}(H{-}CH_2C{\equiv}CH) = -[\Delta H_f(CH_2{=}C{=}CH_2) - \Delta H_f(CH_3C{\equiv}CH)] \quad (24)$$

In this case the heats of formation (Table 1) differ by 1.6 kcal mol^{-1}. Assuming these values are correct,[51] the difference in ΔH_{acid} between allene and methylacetylene also will be 1.6 kcal mol^{-1}. In Table 6 we report $\Delta H_{acid}(CH_2{=}C{=}CH_2)$ = 381.1 $\pm$ 3 kcal mol^{-1}, thus $\Delta H_{acid}(H{-}CH_2C{\equiv}CH)$ = 382.7 $\pm$ 3 kcal mol^{-1}, also reported in Table 6. Our value is in good agreement with the value reported in Table 1 (ΔH_{acid} = 382.3 $\pm$ 1.2 kcal mol^{-1}), derived in an analogous manner. It is also in good agreement with the theoretical value (ΔH_{acid} = 383.2 $\pm$ 2.0 kcal mol^{-1}) reported in Table 2.

Table 7. Bracketing Reactions for $CH_2{=}C{=}\dot{C}^-$ Used in Acidity Evaluation (See Text)

neutral reagent (RH)	$\Delta G_{acid}(RH)$[a]	$\Delta H_{acid}(RH)$[a]	proton abstraction?[b]
CH_3CH_2OH	371.9 $\pm$ 0.8[c]	378.5 $\pm$ 0.8[c]	no
C_7H_8 (cycloheptatriene)	369.2 $\pm$ 2.0	375.2 $\pm$ 2.8	no
C_4H_9OH (*n*-butanol)	368.8 $\pm$ 2.0	375.4 $\pm$ 2.4	no
CH_3CH_2CN	367.4 $\pm$ 2.0	375.1 $\pm$ 2.6	v.s.
$C_5H_{11}OH$ (*n*-pentanol)	367.3 $\pm$ 3.0	373.9 $\pm$ 2.7	no
CH_2Cl_2	366.8 $\pm$ 3.0	374.6 $\pm$ 3.9	no
C_6H_8 (1,3-cyclohexadiene)	365.8 $\pm$ 4.0	373.3 $\pm$ 4.9	no
$CH_2{=}CHCN$	365.3 $\pm$ 2.0	371.1 $\pm$ 2.9	v.s.
CH_3CN	365.2 $\pm$ 2.0	372.9 $\pm$ 2.6	yes
$CH_3C(O)OCH_3$	365.1 $\pm$ 2.0	371.9 $\pm$ 2.3	v.s.
C_6H_5CCH (phenylacetylene)	362.9 $\pm$ 2.0	370.7 $\pm$ 3.2	yes
$CH_3C(O)CH_3$	361.9 $\pm$ 2.0	369.1 $\pm$ 2.6	yes
$CH_3CH_2C(O)CH_2CH_3$	361.4 $\pm$ 2.0	368.6 $\pm$ 2.9	yes
$CH_3CH_2C(O)CH_3$	361.3 $\pm$ 2.0	368.1 $\pm$ 2.9	yes

[a] Reference 32 unless otherwise indicated. Units are kcal mol^{-1}. [b] Ion signal for the proton abstraction product was estimated from product ion spectra. "No" denotes no proton abstraction product was observed, "v.s." denotes a very small (<5%) proton abstraction product was observed, and "yes" denotes proton abstraction was observed as a major product. [c] Table 1 and ref 27.

E. The Gas-Phase Acidity of the Propargyl Radical ($CH_2{=}C{=}\dot{C}{-}H$). Recent results from negative ion photoelectron spectroscopy (PES),[22] in accord with previous PES results,[25] have shown that the reaction between O^- and allene produces only the propadienylidene radical anion:

$$O^- + CH_2{=}C{=}CH_2 \rightarrow CH_2{=}C{=}\dot{C}^- + H_2O \quad (25)$$

In the present study we prepared $CH_2{=}C{=}\dot{C}^-$ according to eq 25, hence we assume that we formed only this isomer. This assumption seems justified, since the only difference between our work and the PES study is that we prepared O^- in a flowing afterglow source using electron impact ionization of N_2O, whereas in the PES study, O^- was prepared in a flowing afterglow source by introducing trace O_2 into a helium microwave discharge.

After preparing the $CH_2{=}C{=}\dot{C}^-$ anion in the first flow tube, we injected it into the second flow tube and examined its reactivity with a variety of reference acids. These data allowed us to bracket the gas-phase acidity of its parent neutral, the propargyl radical ($CH_2{=}C{=}\dot{C}H$). Preliminary results are reported in Table 7, but should be interpreted with caution. In many of the reactions investigated, for example those involving the nitriles (CH_3CH_2CN, $CH_2{=}CHCN$, and CH_3CN) and to a lesser extent the alcohols (C_2H_5OH, n-C_4H_9OH, and n-$C_5H_{11}OH$),

(51) We report the same $\Delta H_f(RH)$ as those used by Oakes and Ellison (ref 23) in their determination of the gas-phase acidity of $CH_2{=}C{=}CH_2$. Their reference was Rosenstock et al. (ref 36). These heats of formation are also in Stull et al. (ref 37). Lias et al. (ref 35) report slightly different values ($\Delta H_f(CH_2{=}C{=}CH_2)$ = 45.6 $\pm$ 0.2 kcal mol^{-1} and $\Delta H_f(CH_3C{\equiv}CH)$ = 44.6 $\pm$ 0.5 kcal mol^{-1}) and cite the following as their source: Pedley, J. B.; Rylance, J. *Sussex—N. P. L. Computer Analysed Thermochemical Data: Organic and Organometallic Compounds*; University of Sussex, 1977. If the values in Lias et al. are correct, the difference in ΔH_{acid} between $CH_2{=}C{=}CH{-}H$ and $H{-}CH_2C{\equiv}CH$ will be 1.0 kcal mol^{-1} rather than 1.6 kcal mol^{-1}.

the total ion signal decreased. The cause of this ion loss is not known, but it may result from an electron detachment process illustrated below for the reactions of $CH_2{=}C{=}\dot{C}^-$ with propionitrile (eq 26) and ethanol (eq 27).

$$CH_2{=}C{=}\dot{C}^- + CH_3CH_2CN \rightarrow CH_2{=}C{=}CH_2 + CH_2{=}CHCN + e^- \quad (26)$$

$$CH_2{=}C{=}\dot{C}^- + CH_3CH_2OH \rightarrow CH_2{=}C{=}CH_2 + CH_3CHO + e^- \quad (27)$$

Similar detachment processes have been observed for other radical anions, e.g., OCC^-.[52] Moreover, in bracketing the acidity of $CH_2{=}C{=}\dot{C}^-$ with various alcohols (ROH), no direct proton transfer products (RO^-) were observed, implying that proton transfer is endoergic, but ions corresponding in mass to adduct ions [$CH_2{=}C{=}\dot{C}^- \cdot ROH$] and cluster ions of the alcohol ([$RO^- \cdot ROH$] and [$RO^- \cdot (ROH)_2$]) were observed. Again, the mechanism for the formation of the alcohol cluster ions is not known, but it may involve a secondary reaction between the observed adduct ion and ROH, as illustrated in eq 28.

$$CH_2CC^- \xrightarrow{ROH} \left[\begin{matrix} CH_2CC^- \\ \bullet \\ ROH \end{matrix}\right] \xrightarrow{\times} RO^- \qquad \left[\begin{matrix} CH_2CC^- \\ \bullet \\ ROH \end{matrix}\right] \xrightarrow{[M]} CH_2CC^- \cdot ROH \xrightarrow{ROH} RO^- \cdot ROH + C_3H_3 \quad (28)$$

Adduct formation and the possibility of electron detachment complicate our ability to bracket the upper limit of the gas-phase acidity of the propargyl radical. An upper limit is typically established where either no or only a minor proton abstraction process is observed, indicating an endoergic reaction pathway. In this case, however, the upper limit may be too small since these additional pathways can, in principle, compete efficiently with exoergic proton abstraction, making it only appear to be an endoergic reaction. Despite these problems, the data in Table 7 do suggest a relatively consistent trend. For gas-phase acidities smaller (more acidic) than phenylacetylene (ΔG_{acid} = 362.9 ± 2.0 kcal mol^{-1}), proton abstraction by $CH_2{=}C{=}\dot{C}^-$ was a major product channel. This suggests a lower limit of $\Delta G_{acid}(CH_2{=}C{=}\dot{C}{-}H)$ of roughly 363 kcal mol^{-1}. Similarly, an upper limit of 366 kcal mol^{-1} can be tentatively established in the reaction with 1,3-cyclohexadiene (ΔG_{acid} = 365.8 ± 4.0 kcal mol^{-1}). We therefore bracket the acidity of the propargyl radical between these two values and estimate $\Delta G_{acid}(CH_2{=}C{=}\dot{C}{-}H)$ = 364 ± 5 kcal mol^{-1}, where the error bars are chosen conservatively to reflect the difficulties in the measurement. Since ΔS_{acid} for the propargyl radical is not known, we estimate $\Delta H_{acid}(CH_2{=}C{=}\dot{C}{-}H)$ by using the values for ΔH_{acid} also reported in Table 7. We again select phenylacetylene for the lower limit (ΔH_{acid} = 370.7 ± 3.2 kcal mol^{-1}) and 1,3-cyclohexadiene for the upper limit (ΔH_{acid} = 373.3 ± 4.9 kcal mol^{-1}) and determine that $\Delta H_{acid}(CH_2{=}C{=}\dot{C}{-}H)$ = 372 ± 5 kcal mol^{-1}. These values are reported in Table 6.

4. Bond Dissociation Energies

We combine the electron affinity measurements given in section 2 with the gas-phase acidity data presented in section 3 to arrive at bond dissociation energies according to the relationship shown in eq 29 and derived from eqs 1−4:

$$D(R{-}H) = \Delta H_{acid}(R{-}H) + EA(R) - IP(H) \quad (29)$$

Table 8 summarizes the values of $D_{298}(R{-}H)$ obtained using eq 29. We cite 298 K values for the bond energies because the gas-phase acidities were measured at 298 K. However, the electron affinities were measured at 0 K. Technically, the 0 K electron affinities should be corrected by the difference of enthalpy differences, $\{[H_{298}(R) - H_0(R)] - [H_{298}(R^-) - H_0(R^-)]\}$, to produce a 298 K electron affinity.[53] This difference is typically less than 0.5 kcal mol^{-1} and can be neglected at our level of precision. Table 8 also contains our values for the heats of formation of the radicals ($\Delta H_f(R)$) resulting from bond dissociation. The first three values in the table include the heats of formation of propargyl ($CH_2{=}C{=}\dot{C}H$ or $\dot{C}H_2C{\equiv}CH$) and 1-propynyl ($CH_3C{\equiv}\dot{C}$) calculated using our BDEs and literature values for the allene, methylacetylene, and hydrogen atom heats of formation. The final value is for propadienylidene ($CH_2{=}C{=}\ddot{C}$), determined using a precise literature value for $\Delta H_f(CH_2{=}C{=}\dot{C}H)$ (which differs from our value by 1 kcal mol^{-1}) along with our experimental BDE.

5. Discussion

Of the bond dissociation energies shown in Table 8, only the first two, involving dissociation to produce the propargyl radical ($CH_2{=}C{=}\dot{C}{-}H$), have been measured previously. It should be noted that because the heats of formation of both allene and methylacetylene are very precisely known, measurement of any one of three energies, the two C−H bond dissociation energies or the heat of formation of the propargyl radical, yields the other two energies. As discussed in the introduction, the $\Delta H_f(CH_2{=}C{=}\dot{C}H)$ has been the subject of very extensive investigation, with a consensus heat of formation of 81.5 ± 1.0 kcal mol^{-1}, an allene ($CH_2{=}C{=}CH{-}H$) bond dissociation energy (BDE) of 87.7 ± 1.0 kcal mol^{-1}, and a methylacetylene ($H{-}CH_2C{\equiv}CH$) BDE of 89.3 ± 1.0 kcal mol^{-1}.[18,19] Our measurements are in excellent agreement with the previous measurements.

The BDE for the acetylenic site of methylacetylene [$D_0(CH_3C{\equiv}C{-}H)$] has not been determined previously. Our value (130.2 ± 3.0 kcal mol^{-1}) is in reasonable agreement with a recent *ab initio* calculation by Bauschlicher and Langhoff[24] (135.9 ± 2 kcal mol^{-1}). The most striking aspect of both the experimental and theoretical values is their similarity to the BDE of acetylene (131.3 ± 0.7 kcal mol^{-1}).[13-15] This is somewhat surprising since the 1-propynyl radical resulting from bond dissociation of methylacetylene ($CH_3C{\equiv}\dot{C}$) has a ^2E ground state, whereas the diabatic asymptote which best corresponds to the acetylene BDE to form ethynyl ($HC{\equiv}\dot{C}$) involves the $^2A_1$ excited state of $CH_3C{\equiv}\dot{C}$ (the ground state of $HC{\equiv}\dot{C}$ is $^2A_1$). Bauschlicher and Langhoff[24] calculate that the $CH_3C{\equiv}\dot{C}$ ^2E ground state lies 9.7 kcal mol^{-1} below the $^2A_1$ first excited state. One might expect that the BDE for methylacetylene would be lowered by the cost of promotion of $CH_3C{\equiv}\dot{C}$ to the $^2A_1$ state. In fact, when the methylacetylene BDE [$D_0(CH_3C{\equiv}C{-}H)$] is referenced to the $^2A_1$ state predicted by the calculations, we obtain a diabatic BDE that is 10 kcal mol^{-1} higher than for acetylene.

Similarly, we have determined the BDE for the acetylenic hydrogen on propargyl radical ($\dot{C}H_2C{\equiv}C{-}H \leftrightarrow CH_2{=}C{=}\dot{C}{-}H$) to be 100 ± 5 kcal mol^{-1}. This adiabatic dissociation is to the singlet ground state of propadienylidene ($CH_2{=}C{=}\ddot{C}$). The

(52) Van Doren, J. M.; Miller, T. M.; Miller, A. E. S.; Viggiano, A. A.; Morris, R. A.; Paulson, J. F. *J. Am. Chem. Soc.* **1993**, *115*, 7407.

(53) Janz, G. J. *Estimation of Thermodynamic Properties of Organic Compounds*; Academic Press: New York, 1958.

Table 8. Derived C−H Bond Dissociation Energies [D_{298}(R−H) = ΔH_{acid}(R−H) + EA(R) − IP(H)] and Radical Heats of Formation [ΔH_f(R) = ΔH_f(RH) − ΔH_f(H) + D_{298}(RH)]

compd (R−H)	$\Delta H_{acid(298)}$(R−H) (kcal mol^{-1})	EA(R) (eV)	D_{298}(R−H)[a] (kcal mol^{-1})	ΔH_f(R)[b] (kcal mol^{-1})
CH_2=C=CH−H	381.1 ± 3	0.918 ± 0.008	88.7 ± 3	82.5 ± 3
H-CH_2C≡CH	382.7 ± 3	0.918 ± 0.008	90.3 ± 3	82.5 ± 3
CH_3C≡C−H	381.1 ± 3	2.718 ± 0.008	130.2 ± 3	122.4 ± 3
CH_2=C=Ċ−H	372 ± 5	1.794 ± 0.008	100 ± 5	129.4 ± 4

[a] Uses 23.0604 kcal mol^{-1} = 1 eV and IP(H) = 313.5874 kcal mol^{-1}. Neglects electron affinity conversion from 0 to 298 K. [b] Uses ΔH_f(RH) from Table 1, ΔH_f(H) = 52.103 kcal mol^{-1}, and D_{298}(R−H) from this work. For the last row we use ΔH_f(CH_2=C=ĊH) = 81.5 ± 1.0 kcal mol^{-1} (ref 19).

diabatic process which corresponds more closely to bond dissociation in acetylene will leave behind an unpaired electron in the σ orbital associated with the C−H bond, yielding the triplet excited state. This diabatic dissociation energy is given by the sum of the adiabatic BDE and the triplet promotion energy (both determined in this work), 100 kcal mol^{-1} + 29.66 kcal mol^{-1} = 130 kcal mol^{-1}. As might be expected, this is equal to a nominal acetylenic C−H bond dissociation energy. An argument has recently been advanced by Clauberg et al.[54] to suggest that the sum of the propadienylidene (CH_2=C=C̈) singlet−triplet splitting and the propargyl BDE [D_0(CH_2=C=Ċ−H)] should be equal to a nominal acetylenic BDE. The argument was then used to predict a propadienylidene singlet−triplet splitting of 40 kcal mol^{-1}. While our data clearly validate the basic argument, it is also clear that the singlet−triplet splitting prediction is in error, primarily because an experimental measurement of the propargyl BDE was not available. The measured singlet−triplet splitting is also in excellent agreement with a recent *ab initio* calculation by Jonas, Bohme, and Frenking,[55] treating the C_3H_2 hypersurface at the highest level to date. Calculations at the PMP4/6-31G(d)//MP2/6-31G(d) level predict a singlet−triplet splitting of 30 kcal mol^{-1}.

Acknowledgment. We gratefully acknowledge Robert F. Gunion for his help in collecting data for the liquid nitrogen cooled spectra of the allenyl anion and Christopher Hadad for his assistance in calculating theoretical gas-phase acidities. W.C.L. acknowledges financial assistance from the National Science Foundation under Grant Nos. CHEM 93-18639 and PHY 90-12244. C.H.D. acknowledges financial support from the Petroleum Research Fund, administered by the American Chemical Society under Grant No. 24223-AC4. V.M.B. acknowledges support from the National Science Foundation under Grant No. CHE-9121781.

JA944139J

(54) Clauberg, H.; Minsek, D. W.; Chen, P. *J. Am. Chem. Soc.* **1992**, *114*, 99.

(55) Jonas, V.; Bohme, M.; Frenking, G. *J. Phys. Chem.* **1992**, *96*, 1640.